

1 Evidence of high N₂ fixation rates in the temperate Northeast 2 Atlantic

3
4 Debany Fonseca-Batista^{1,2}, Xuefeng Li^{1,3}, Virginie Riou⁴, Valérie Michotey⁴, Florian Deman¹,
5 François Fripiat⁵, Sophie Guasco⁴, Natacha Brion¹, Nolwenn Lemaitre^{1,6,7}, Manon Tonnard^{6,8},
6 Morgane Gallinari⁶, Hélène Planquette⁶, Frédéric Planchon⁶, Géraldine Sarthou⁶, Marc Elskens¹,
7 Julie LaRoche², Lei Chou³, Frank Dehairs¹

8
9 ¹ Analytical, Environmental and Geo-Chemistry, Earth System Sciences Research Group, Vrije Universiteit Brussel,
10 1050 Brussels, Belgium

11 ² Department of Biology, Dalhousie University, Halifax, Nova Scotia, Canada B3H 4R2

12 ³ Service de Biogéochimie et Modélisation du Système Terre - Océanographie Chimique et Géochimie des Eaux,
13 Université Libre de Bruxelles, 1050 Brussels, Belgium

14 ⁴ Aix-Marseille Univ, Université de Toulon, CNRS, IRD, MIO, Marseille, France

15 ⁵ Max Planck Institute for Chemistry, Climate Geochemistry Department, 55128 Mainz, Germany

16 ⁶ Laboratoire des Sciences de l'Environnement MARin – CNRS UMR 6539 – Institut Universitaire Européen de la
17 Mer, 29280 Plouzané, France

18 ⁷ Department of Earth Sciences, Institute of Geochemistry and Petrology, ETH-Zürich, 8092 Zürich, Switzerland

19 ⁸ Institute for Marine and Antarctic Studies, University of Tasmania, Hobart, TAS 7001, Australia

20

21 *Correspondence to:* Debany Fonseca P. Batista (dbatista8@hotmail.com)

22 **Abstract.** Diazotrophic activity and primary production (PP) were investigated along two transects (Belgica
23 BG2014/14 and GEOVIDE cruises) off the western Iberian Margin and the Bay of Biscay in May 2014. We report
24 substantial N₂ fixation activities at 8 of the 10 stations sampled, ranging overall between 81 and 384 μmol N m⁻² d⁻¹
25 (0.7 to 8.2 nmol N L⁻¹ d⁻¹), with two sites close to the Iberian Margin between 38.8° N and 40.7° N yielding rates
26 reaching up to 1355 and 1533 μmol N m⁻² d⁻¹. Primary production was relatively lower along the Iberian Margin with
27 rates ranging from 33 to 59 mmol C m⁻² d⁻¹, while it increased towards the northwest away from the Peninsula,
28 reaching as high as 135 mmol C m⁻² d⁻¹. Our observations in combination with area-averaged Chl *a* satellite data,
29 contemporaneous with our study period, revealed that post-bloom conditions prevailed at most sites, while at the
30 northwesternmost station the bloom was still ongoing. When converted to carbon uptake using Redfield
31 stoichiometry, we find that N₂ fixation rates could have supported 1 to 3% of euphotic layer daily PP at most sites,
32 except at the two most active sites where this contribution to daily PP could reached as high as 25%. At the two sites
33 where N₂ fixation activity was highest, *nifH* sequences assigned to the prymnesiophyte-symbiont *Candidatus*
34 *Atelocyanobacterium thalassa* (UCYN-A) dominated the *nifH* sequence pool recovered from DNA samples, while the
35 remaining sequences belonged to non-cyanobacterial phylotypes. At all the other sites where *nifH* sequences were
36 recovered, these belonged exclusively to non-cyanobacterial phylotypes. We support that the unexpectedly high N₂
37 fixation activities recorded at the time of our study were promoted by the availability of phytoplankton-derived
38 organic matter produced during the spring bloom, as evidenced by the significant surface particulate organic carbon
39 concentrations, and also sustained by the presence of excess phosphorus signature in surface waters, particularly at
40 the sites with extreme activities. Our findings stress the need for a more detailed monitoring of oceanic N₂ fixation in
41 productive waters of the temperate North Atlantic to better constrain nitrogen input to the Atlantic Ocean inventory.

42

43 **1 Introduction**

44 Dinitrogen (N₂) fixation is the major pathway of nitrogen (N) input to the global ocean and thereby contributes to
45 sustaining oceanic primary productivity (Falkowski, 1997). The conversion by N₂-fixing micro-organisms
46 (diazotrophs) of dissolved N₂ gas into bioavailable nitrogen also contributes to new production in the euphotic layer
47 and as such, to the subsequent sequestration of atmospheric carbon dioxide into the deep ocean (Gruber, 2008).
48 Estimating the overall contribution of N₂ fixation to carbon sequestration in the ocean requires an assessment of the
49 global marine N₂ fixation.

50 Until recently most studies of N₂ fixation have focused on the tropical and subtropical regions of the global ocean,
51 with few attempts to measure N₂ fixation at higher latitudes, with the exception of enclosed brackish seas
52 (Ohlendieck et al., 2000; Luo et al., 2012; Farnelid et al., 2013). The intense research effort in the low latitude
53 regions stem for the observable presence of cyanobacterial diazotrophs such as the diatom-diazotroph association
54 (DDA) and the colony-forming filamentous *Trichodesmium* (Capone, 1997; Capone et al., 2005; Foster et al., 2007).
55 *Trichodesmium* in particular, long considered as the most active diazotroph in the global ocean, has mostly been
56 reported in oligotrophic tropical and subtropical oceanic waters, thought to represent the optimal environment for its
57 growth and N₂-fixing activity (Dore et al., 2002; Breitbarth et al., 2007; Montoya et al., 2007; Needoba et al., 2007;
58 Moore et al., 2009; Fernández et al., 2010; Snow et al., 2015). In low latitude regions, warm, stratified surface waters
59 depleted in dissolved inorganic nitrogen (DIN), are assumed to give a competitive advantage to diazotrophs over
60 other phytoplankton since only they can draw N from the unlimited dissolved N₂ pool for their biosynthesis. As such,
61 past estimates of global annual N₂ fixation were mainly based on information gathered from tropical and subtropical
62 regions, while higher latitude areas have been poorly explored for diazotrophic activity (Luo et al., 2012).

63 Studies using genetic approaches targeting the *nifH* gene encoding the nitrogenase enzyme, essential for diazotrophy,
64 have shown the presence of diverse diazotrophs throughout the world's oceans, extending their ecological niche
65 (Farnelid et al., 2011; Cabello et al., 2015; Langlois et al., 2015). Small diazotrophs such as unicellular diazotrophic
66 cyanobacteria (UCYN classified in groups A, B and C) and non-cyanobacterial diazotrophs, mostly heterotrophic
67 bacteria (e.g. Alpha- and Gammaproteobacteria), have been observed over a wide range of depth and latitude, thereby
68 expanding the potential for diazotrophy to a much broader geographic scale (Langlois et al., 2005, 2008; Krupke et
69 al., 2014; Cabello et al., 2015). The discovery of a methodological bias associated to the commonly used ¹⁵N₂ bubble-
70 addition technique (Mohr et al., 2010) and the presence of an abundant diazotrophic community in high latitude
71 regions actively fixing N₂ (Needoba et al., 2007; Rees et al., 2009; Blais et al., 2012; Mulholland et al., 2012;
72 Shiozaki et al., 2015), indicate that more efforts are needed to better constrain oceanic N₂ fixation and diazotrophic
73 diversity at higher latitudes.

74 In the Northeast Atlantic, the large input of iron-rich Saharan dust alleviating dissolved iron (dFe) limitation of the
75 nitrogenase activity (Fe being a co-factor of the N₂-fixing enzyme) (Raven, 1988; Howard & Rees, 1996; Mills et al.,
76 2004; Snow et al., 2015) and the upwelling of subsurface waters with low DIN (dissolved inorganic nitrogen) to
77 phosphate ratios, make this region highly favorable for N₂ fixation activity (Deutsch et al., 2007; Moore et al., 2009).
78 In addition, the northeast Atlantic has been observed to harbour a highly active and particularly diverse diazotrophic
79 community (Langlois et al., 2008; Moore et al., 2009; Großkopf et al., 2012; Ratten et al., 2015; Fonseca-Batista et
80 al., 2017) not only in the tropical and subtropical regions but also in the temperate Iberian region which was reported
81 to be a hotspot of prymnesiophyte-UCYN-A symbiotic associations at the global ocean scale (Cabello et al., 2015).
82 Earlier studies in the Iberian open waters investigated the diazotrophic activity either during stratified water column
83 conditions of boreal summer and autumn (Moore et al., 2009; Benavides et al., 2011; Snow et al., 2015; Fonseca-
84 Batista et al., 2017) or during winter convection period (Rijkenberg et al., 2011; Agawin et al., 2014). Here, we

85 present N₂ fixation rate measurements and the taxonomic affiliation of the diazotrophic community from two
86 consecutive missions carried out in the Northeast sector of the Atlantic Ocean in May 2014, during and after the
87 spring bloom.

88 **2 Material and Methods**

89 **2.1 Site description and sample collection**

90 Field experiments were conducted during two nearly simultaneous cruises in May 2014. The Belgica BG2014/14
91 cruise (21–30 May 2014, R/V *Belgica*), investigated the Bay of Biscay and the western Iberian Margin. In parallel,
92 the GEOVIDE expedition in the framework of the international GEOTRACES program (GA01 section, May 16 to
93 June 29 2014, R/V *Pourquoi pas?*) sailed from the Portuguese shelf area towards Greenland and ended in
94 Newfoundland, Canada (<http://dx.doi.org/10.17600/14000200>). For the latter expedition, only four stations within the
95 Iberian Basin investigated for N₂ fixation activity (stations Geo-1, 2, 13 and 21) are considered in this paper and the
96 measurements are compared with those conducted at the six sites studied during the BG2014/14 cruise (stations Bel-
97 3, 5, 7, 9, 11 and 13; Fig. 1).

98 All sampling sites were located within the Iberian Basin Portugal Current System (PCS) (Ambar and Fiúza, 1994)
99 which is influenced by highly fluctuating wind stresses (Frouin et al., 1990). The predominant upper layer water mass
100 in this basin is the Eastern North Atlantic Central Water (ENACW), a winter mode water which according to Fiúza
101 (1984) consists of two components (see θ/S diagrams in Supporting Information Fig. S1): (i) the lighter, relatively
102 warm (> 14°C) and salty (> 35.6) ENACW_{st} formed in the subtropical Azores Front region (~35° N) when Azores
103 Mode Water is subducted as a result of strong evaporation and winter cooling; and (ii) the colder and less saline
104 ENACW_{sp}, underlying the ENACW_{st}, and formed in the subpolar eastern North Atlantic (north of 43° N) through
105 winter cooling and deep convection (McCartney and Talley, 1982). The spatial distribution of these Central Waters
106 allowed categorizing the sampling sites in 2 groups: (i) ENACW_{sp} stations north of 43° N (Bel-3, Bel-5, Bel-7, and
107 Geo-21) only affected by the ENACW_{sp} (Fig. S1a, b) and (ii) ENACW_{st} stations, south of 43° N, characterized by
108 the upper layer being influenced by ENACW_{st} and the subsurface layer by ENACW_{sp} (Fig. S1a, b). Most of these
109 ENACW_{st} stations were open ocean sites (Bel-9, Bel-11, Bel-13, and Geo-13) while two stations were in proximity
110 of the Iberian shelf (Geo-1 and Geo-2) (Tonnard et al., 2018).

111 Temperature, salinity and photosynthetically active radiation (PAR) profiles down to 1500 m depth were obtained
112 using a conductivity-temperature-depth sensor (SBE 09 and SBE 911+, during the BG2014/14 and GEOVIDE
113 cruises, respectively) fitted to rosette frames. For all biogeochemical measurements seawater samples were collected
114 from Niskin bottles attached to the rosette and triggered at specific depths in the upper 200 m. In particular, for stable
115 isotope incubation experiments seawater was collected in 4.5 L acid-cleaned polycarbonate (PC) bottles from four
116 depths corresponding to 54%, 13%, 3% and 0.2% of surface PAR at stations Bel-3, 5, 7, 9, 11, and Geo-2. At stations
117 Geo-1, 13 and 21, two additional depths corresponding to 25% and 1% of surface PAR were also sampled for the
118 same purpose.

119

120 **2.2 Nutrient measurements**

121 Surface water concentrations of ammonium (NH₄⁺) during both cruises were measured on board as well as nitrate +
122 nitrite (NO₃⁻ + NO₂⁻) concentrations during the GEOVIDE expedition. During the BG2014/14 cruise, samples for

123 $\text{NO}_3^- + \text{NO}_2^-$ and phosphate (PO_4^{3-}) measurements were filtered (0.2 μm) and stored at -20°C until analysis at the
 124 home-based laboratory. PO_4^{3-} data are not available for the GEOVIDE cruise.
 125 Nutrient concentrations were determined using the conventional fluorometric (for NH_4^+) (Holmes et al., 1999) and
 126 colorimetric methods (for the other nutrients) (Grasshoff et al., 1983) with detection limits (DL) of 64 nmol L^{-1}
 127 (NH_4^+), 90 nmol L^{-1} ($\text{NO}_3^- + \text{NO}_2^-$) and 60 nmol L^{-1} (PO_4^{3-}). For the BG2014/14 cruise, chlorophyll *a* (Chl *a*)
 128 concentrations were determined according to Yentsch and Menzel (1963), by filtering 250 mL of seawater sample
 129 onto Whatman GF/F glass microfiber filters (0.7 μm nominal pore size), followed by pigment extraction in 90%
 130 acetone, centrifugation and fluorescence measurement using a Shimadzu RF-150 fluorometer.
 131

132 2.3 $^{15}\text{N}_2$ fixation and $^{13}\text{C}\text{-HCO}_3^-$ uptake rates

133 N_2 fixation and primary production (PP) were determined simultaneously from the same incubation sample in
 134 duplicate using the $^{15}\text{N}\text{-N}_2$ dissolution method (Großkopf et al., 2012) and $^{13}\text{C}\text{-NaHCO}_3$ tracer addition (Hama et al.,
 135 1983) techniques, respectively. Details concerning the applied $^{15}\text{N}_2$ dissolution method can be found in Fonseca-
 136 Batista et al. (2017). Briefly, $^{15}\text{N}_2$ -enriched seawater was prepared by degassing prefiltered (0.2 μm) low nutrient
 137 seawater, thereafter stored in 2 L gastight Tedlar bags (Sigma-Aldrich) subsequently injected with 30 mL of pure
 138 $^{15}\text{N}_2$ gas (98 ^{15}N atom%, Eurisotop, lot number 23/051301) and left to equilibrate. This $^{15}\text{N}_2$ gas batch (Eurisotop) has
 139 previously been shown to be free of ^{15}N -labelled contaminants such as nitrate, nitrite, ammonium and nitrous oxide.
 140 Each PC incubation bottle was partially filled with sampled seawater, then amended with 250 mL of $^{15}\text{N}_2$ -enriched
 141 seawater, spiked with 3 mL of a $\text{NaH}^{13}\text{CO}_3$ solution (200 mmol L^{-1} , 99%, Eurisotop) and topped off with the original
 142 seawater sample. Samples were incubated for 24 hours in on-deck incubators circulated with surface seawater and
 143 wrapped with neutral density screens (Rosco) simulating the in situ irradiance conditions. After incubation, samples
 144 were filtered onto pre-combusted MGF filters (glass microfiber filters, 0.7 μm nominal pore size, Sartorius), which
 145 were subsequently dried at 60°C and stored at room temperature. The natural concentration and isotopic composition
 146 of particulate organic carbon and particulate nitrogen (POC and PN) were assessed by filtering an additional 4.5 L of
 147 non-spiked seawater from each depth. All samples were measured for POC and PN concentrations and isotopic
 148 compositions using an elemental analyzer (EuroVector Euro EA 3000) coupled to an isotope ratio mass spectrometer
 149 (Delta V Plus, Thermo Scientific) and calibrated against international certified reference materials (CRM): IAEA-N1
 150 and IAEA-305B for N and IAEA-CH6 and IAEA-309B for C. N_2 fixation and carbon uptake volumetric rates were
 151 computed as shown in Equation 1:

$$152 \text{N}_2 \text{ or } \text{HCO}_3^- \text{ uptake rate (nmol L}^{-1}\text{d}^{-1} \text{ or } \mu\text{mol m}^{-3}\text{d}^{-1}) = \frac{A_{\text{PN or POC}}^{\text{final}} - A_{\text{PN or POC}}^{t=0}}{A_{\text{N}_2 \text{ or DIC}} - A_{\text{PN or POC}}^{t=0}} \times \frac{[\text{PN or POC}]}{\Delta t} \quad (1)$$

153 where *A* represents the ^{15}N or ^{13}C atom% excess of PN or POC at the beginning ($t=0$) and end (final) of the
 154 incubation, or of the dissolved inorganic pool (N_2 or dissolved inorganic carbon, DIC); and Δt the incubation period.
 155 Depth-integrated rates were calculated by non-uniform gridding trapezoidal integration for each station. Minimal
 156 detectable uptake rates were determined as detailed in Fonseca-Batista et al. (2017). To do so, the minimal acceptable
 157 ^{15}N or ^{13}C enrichment of PN or POC after incubation (Montoya et al., 1996) is considered to be equal to the natural
 158 isotopic composition, specific to each sampled depth, increased by three times the uncertainty obtained for N and C
 159 isotopic analysis of CRM. All remaining experiment-specific terms are then used to recalculate the minimum
 160 detectable uptake. Carbon uptake rates were always above their specific DL, while N_2 fixation was undetectable for
 161 some incubations (see details in section 3.3).

162

163 2.4 DNA sampling and *nifH* diversity analysis

164 During the BG2014/14 and GEOVIDE cruises water samples were also collected for DNA extraction and *nifH*
165 sequencing at the stations where N₂ fixation rate measurements were carried out, prior to incubation. 2 L volumes
166 were vacuum filtered (20 to 30 kPa) through 0.2 µm sterile cellulose acetate filters (47 mm Sartorius type 111)
167 subsequently placed in cryovials directly flash deep frozen in liquid nitrogen. At the land-based laboratory samples
168 were transferred to a -80°C freezer until nucleic acid extraction.

169 For the BG2014/14 samples, DNA was extracted from the samples using the Power Water DNA Isolation kit
170 (MOBIO) and checked for integrity by agarose gel electrophoresis. The amplification of *nifH* sequences was
171 performed on 3–50 ng µL⁻¹ environmental DNA samples using one unit of Taq polymerase (5PRIME), by nested
172 PCR according to Zani et al. (2000) and Langlois et al. (2005). Amplicons of the predicted 359-bp size observed by
173 gel electrophoresis were cloned using the PGEM T Easy cloning kit (PROMEGA) according to the manufacturer's
174 instructions. A total of 103 clones were sequenced by the Sanger technique (GATC, Marseille).

175 For the GEOVIDE samples, DNA was extracted using the QIAGEN DNeasy Plant Mini Kit as directed by the
176 manufacture, with a modified step to improve cell lysis. This step consisted of an incubation at 52°C on an orbital
177 shaker for 1 hour (300 rpm) with 50 µL of lysozyme solution (5 mg mL⁻¹ in TE buffer), 45 µL of Proteinase K
178 solution (20 mg mL⁻¹ in MilliQ PCR grade water) and 400 µL of API lysis buffer from the QIAGEN DNeasy Plant
179 Mini Kit. DNA concentration and purity were assessed with NanoDrop 2000 and then stored at -80 °C. The DNA
180 samples were screened for the presence of the *nifH* gene as described in Langlois et al. (2005). Samples that tested
181 positive were further prepared for next generation sequencing on an Illumina MiSeq platform using primers that
182 included the *nifH*1/2 primers (Langlois et al., 2005; Ratten, 2017) attached to Illumina adaptors and barcodes for
183 multiplexing in the Illumina MiSeq instrument. Next generation sequencing was carried out at the Integrated
184 Microbiome Resource (IMR) of the Centre for Comparative and Evolutionary Biology (CGEB) at Dalhousie
185 University (Halifax, Canada). Raw Illumina paired-end reads of *nifH* were preprocessed using the QIIME pipeline
186 (Quantitative Insights Into Microbial Ecology; Caporaso et al., 2010) using the IMR workflow
187 (https://github.com/mlangill/microbiome_helper/wiki/16S-standard-operating-procedure; Comeau et al., 2017). The
188 28 OTUs for the *nifH* genes presented in this study were assembled based on 96% identity of sequence reads.

189 DNA alignments were performed using the Molecular Evolutionary Genetics Analysis software (MEGA 7.0) (Kumar
190 et al., 2016) and *nifH* operational taxonomic units (*nifH*-OTUs) were defined with a maximum 5% divergence cut-
191 off. DNA sequences were translated into amino acid sequences, then *nifH* evolutionary distances which are
192 considered as the number of amino acid substitutions per site, were computed using the Poisson correction method
193 (Nei, 1987). All positions containing gaps and missing data were eliminated (see phylogenetic tree in Fig. 6). One
194 sequence of each *nifH*-OTU was deposited in GenBank under the accession numbers referenced from KY579322 to
195 KY579337, for the Belgica DNA samples and referenced from MH974781 to MH974795 for the GEOVIDE Iberian
196 samples.

197

198 2.5 Statistical analysis

199 In order to examine the relationship between N₂ fixation activities and ambient physical and chemical properties,
200 using SigmaPlot (Systat Software, San Jose, CA) we computed Spearman rank correlation coefficients linking depth-
201 integrated rates and volumetric rates of N₂ fixation and primary production to environmental variables either
202 averaged or integrated over the euphotic layer, or measured in a discrete manner, respectively. These variables
203 include temperature, salinity, Chl *a*, NH₄⁺, NO₃⁻+NO₂⁻, phosphorus excess ($P^* = [PO_4^{3-}] - [NO_3^- + NO_2^-] / 16$)

204 derived from in situ nutrient measurements and climatological data (Garcia et al., 2013), dissolved iron
205 concentrations determined for the GEOVIDE cruise (Tonnard et al., 2018) and satellite-derived dust deposition fluxes
206 at the time of our study (Giovanni online data system). When nutrient concentrations were below the DL we used the
207 DL value to run the correlation test. In addition, we also ran a principal component analysis; using XLSTAT 2017
208 (Addinsoft, Paris, France, 2017) to get an overview of the interconnection between all the latter key variables with N₂
209 fixation at the time of our study. The output of the PCA are discussed in section 4.3.

210 **3 Results**

211 **3.1 Ambient environmental settings**

212 Surface waters of all the ENACWst stations showed a relatively strong stratification resulting from the progressive
213 spring heating, with sea surface temperature (SST) ranging from 15.3 (Geo-13) to 17.2°C (Bel-13). Nutrients were
214 depleted at the surface ($\text{NO}_3^- + \text{NO}_2^- < 0.09 \mu\text{M}$ in the upper 20 m; Fig. 2c, f) and surface Chl *a* concentrations were
215 low ($< 0.25 \mu\text{g L}^{-1}$; Fig. 2a, d) but showed a subsurface maximum (between 0.5 and $0.75 \mu\text{g L}^{-1}$ at approximately 50
216 m), a common feature for oligotrophic open ocean waters. Amongst the ENACWst stations, station Geo-13 had a
217 slightly higher nutrient content ($\text{NO}_3^- + \text{NO}_2^- = 0.7 \mu\text{M}$ in the lower mixed layer depth, MLD) and higher Chl *a* ($>$
218 $0.5 \mu\text{g L}^{-1}$ in the upper 35 m).

219 Surface waters at ENACWsp stations were less stratified (SST between 14.0 and 14.5°C), were nutrient replete
220 (surface $\text{NO}_3^- + \text{NO}_2^-$ ranging from 0.3 to $0.8 \mu\text{M}$) and had a higher phytoplankton biomass (Chl *a* between 0.7 to 1.2
221 $\mu\text{g L}^{-1}$ in the upper 30 m except for station Bel-5). Highest Chl *a* values were observed at station Bel-7 (44.6°N , 9.3°
222 W), which appeared to be located within an anticyclonic mesoscale eddy, as evidenced by the downwelling structure
223 detected in the Chl *a* and $\text{NO}_3^- + \text{NO}_2^-$ profiles (Fig. 2a, c) at this location (as well as T and S sections, data not
224 shown).

225

226 **3.2 Primary production and satellite-based chl *a* observations**

227 Primary production (PP), estimated through the incorporation of enriched bicarbonate ($^{13}\text{C-NaHCO}_3$) into the
228 particulate organic carbon (POC) pool, illustrated volumetric rates ranging from 7 to $3500 \mu\text{mol C m}^{-3} \text{d}^{-1}$ (see
229 Supporting Information Table S1) and euphotic layer integrated rates ranging from 32 to $137 \text{mmol C m}^{-2} \text{d}^{-1}$ (Fig.
230 3a, b, and Supporting Information Table S2). PP was relatively homogenous in the Bay of Biscay (stations Bel-3,
231 Bel-5 and Bel-7) and along the Iberian Margin (Bel-9, Bel-11, Bel-13 and Geo-1) with average rates ranging from 33
232 to $43 \text{mmol C m}^{-2} \text{d}^{-1}$, except at station Bel-7 where it was slightly higher ($52 \text{mmol C m}^{-2} \text{d}^{-1}$; Fig. 3a, b, and Table
233 S2), likely due to the presence of an anticyclonic mesoscale structure at this location. PP increased westwards away
234 from the Iberian Peninsula, reaching highest values at stations Geo-13 and Geo-21 (79 and $135 \text{mmol C m}^{-2} \text{d}^{-1}$,
235 respectively; Fig. 3b) as well as closer to the shelf (reaching $59 \text{mmol C m}^{-2} \text{d}^{-1}$ at Geo-2). These results are in the
236 range of past measurements in this region for the same period of the year, ranging from 19 to $103 \text{mmol C m}^{-2} \text{d}^{-1}$
237 (Marañón et al., 2000; Fernández et al., 2005; Poulton et al., 2006; Fonseca-Batista et al., 2017). Area-averaged Chl *a*
238 derived from satellite imagery for a time-period overlapping with our (Giovanni online data system; Fig. 4a, b)
239 revealed that post-bloom conditions prevailed at most sites (Bel-3 to Bel-13 and Geo-1 to Geo-13) while bloom
240 conditions were still found at station Geo-21 at the time of our study.

241

242 3.3 N₂ fixation and dominant diazotrophs at the sampling sites

243 Volumetric N₂ fixation rates were above the detection limit at 8 of the 10 stations sampled in this study (excluding
244 Bel-3 and Bel-5 where rates were below the detection limit) and ranged from 0.7 to 65.4 nmol N L⁻¹ d⁻¹ (see Table
245 S1), with areal rates ranging between 81 and 1533 μmol N m⁻² d⁻¹ (Fig. 3c, d, and Table S2).

246 We observed intense N₂ fixation activities at the two sites (Bel-11 and Bel-13) most affected by ENACW waters of
247 subtropical origin (Fig. S1). At stations Bel-11 and Bel-13, volumetric rates of N₂ fixation ranged from 2.4 to 65.4
248 nmol N L⁻¹ d⁻¹, with highest rates found at surface level (65.4 and 45.0 nmol N L⁻¹ d⁻¹, respectively), while areal rates
249 averaged 1533 and 1355 μmol N m⁻² d⁻¹, respectively. N₂ fixation was detected at all four GEOVIDE stations. Shelf-
250 influenced (Geo-1 and Geo-2) and open ocean (Geo-13) ENACWst sites, geographically close to Bel-11 and Bel-13,
251 also displayed high N₂ fixation activities with volumetric rates ranging between 1.0 and 7.1 nmol N L⁻¹ d⁻¹ (Table S1)
252 while depth-integrated rates averaged 141, 262 and 384 μmol N m⁻² d⁻¹, respectively (Fig. 3c, d, and Table S2).
253 Significant N₂ fixation rates were also measured at stations that overall exhibited the highest primary production
254 rates, including Bel-7, Geo-13 and Geo-21 (Fig. 3). We computed the relative contribution of N₂ fixation to PP by
255 converting N₂ fixation rates to carbon uptake using either a Redfield ratio of 6.6 or the determined median POC/PPN
256 ratio for natural particles (equivalent to the mean value of 6.3 ± 1.1, ± SD, n = 46; Table 1). N₂ fixation contributed to
257 less than 2% of PP at the ENACWsp sites Bel-7 and Geo-21 and between 3 to 28% of PP at the ENACWst sites,
258 except at station Bel-9 where it supported about 1% of PP.

259 Screening of the *nifH* genes from DNA samples collected during the BG2014/14 cruise, returned positive *nifH*
260 presence at stations Bel-11 and Bel-13 that displayed the largest areal N₂ fixation rates. Cloning of the *nifH*
261 amplicons found in surface waters (54% PAR level where volumetric rates of N₂ fixation were highest) yielded 103
262 *nifH* sequences. No successful *nifH* amplifications were obtained at the other Belgica stations or depths where
263 diazotrophic activities were lower or undetectable. All of the clones (n = 41) recovered from station Bel-11 were
264 regrouped in a single OTU that had 99% similarity at the nucleotide level and 100% similarity at the amino acid level
265 with the symbiotic diazotrophic cyanobacteria UCYN-A1 or *Candidatus Atelocyanobacterium thalassa*, first
266 characterized from station ALOHA in the North Pacific (Fig. 5a and 6) (Thompson et al., 2012). While the UCYN-A
267 OTU also dominated the clones recovered from station Bel-13, fourteen additional *nifH* phylotypes affiliated with
268 non-cyanobacterial diazotrophs were also recovered at that station (Fig. 5a and 6). Among these 15 OTUs,
269 represented by a total of 62 sequenced clones, 45.2% of the sequences were affiliated to UCYN-A1 (identical to those
270 found at Bel-11), and the rest to heterotrophic bacteria with 25.8% affiliated to Bacteroidetes, 19.3% to Firmicutes
271 and 9.7% to Proteobacteria (Gamma-, Epsilon- and Deltaproteobacteria; Fig. 5a and 6). For the GEOVIDE cruise,
272 *nifH* screening returned positive *nifH* presence at stations Geo-2, Geo-13 and Geo-21. Next generation sequencing of
273 these amplicons yielded in total 21001 reads, with a range of 170 to 9239 *nifH* amplicons per sample, belonging
274 exclusively to non-cyanobacterial diazotrophs, with the major affiliation to Verrucomicrobia, and Gamma-, Delta-
275 and Alpha-proteobacteria, representing 54, 28, 15 and 1% of total *nifH* amplicons, respectively (Fig. 5b and 6).
276 Members of a clade that has been recently characterized from the TARA expedition through metagenome
277 reconstructed genomes of marine heterotrophic diazotrophs (Delmont et al., 2018), were found among the
278 Gammaproteobacteria OTU types that dominated the community at station Geo-21.

279

280 3.4 Relationship between N₂ fixation rates and environmental variables

281 N₂ fixation activities were measured in surface waters characterized by relatively low SST (12.5–17.3°C) and a wide
282 range of dissolved inorganic nitrogen (DIN) concentrations (NO₃⁻ + NO₂⁻ from < 0.1 to 7.6 μM). Water column

283 integrated N_2 fixation tended to increase with the average surface water salinity ($n = 10$, $p < 0.05$, Table S3) but was
284 inversely correlated to satellite-based dust deposition in May 2014, the month during which our sampling took place
285 ($n = 10$, $p < 0.01$). Volumetric rates of N_2 fixation tended to increase with temperature ($n = 46$, $p < 0.01$, Table S4)
286 and excess phosphorus concentration (only available Belgica studied sites, $n = 24$, $p < 0.01$) while being negatively
287 correlated to nitrate plus nitrite concentration ($n = 46$, $p < 0.01$).

288 **4 Discussion**

289 During two quasi simultaneous expeditions to the Iberian Basin and the Bay of Biscay in May 2014 (38.8–46.5° N),
290 we observed N_2 fixation activity in surface waters of most stations (except at the two northernmost sites in the Bay of
291 Biscay). Our results are in support of other recent studies, that have observed diazotrophic communities and
292 significant N_2 fixation rates in marine environments that depart from the previously established belief that
293 diazotrophs are preferentially associated with warm oceanic water and low fixed-nitrogen concentrations (Needoba et
294 al., 2007; Rees et al., 2009; Blais et al., 2012; Mulholland et al., 2012; Shiozaki et al., 2015). Although there is
295 growing evidence that diazotrophs and their activity extend geographically to temperate coastal and shelf-influenced
296 regions, there are still very few rate measurements at higher latitudes, especially in open waters. In the following
297 sections (1) we discuss the significance of N_2 fixation in the Iberian Basin, its relation to primary productivity pattern
298 and extend our view to the whole Atlantic Ocean, (2) we provide information on the taxonomic affiliation of
299 diazotrophs that were present at the time of our study, and (3) we explore potential environmental conditions that
300 may have supported this unexpectedly high diazotrophic activity in the Iberian Basin.

301

302 **4.1 Significance of N_2 fixation in the temperate ocean**

303 In the present study, we found surprisingly high N_2 fixation activities at most of the studied sites. Rates were
304 exceptionally elevated at two open ocean sites located between 38.8–40.7° N at about 11° W (averaging 1533 and
305 1355 $\mu\text{mol N m}^{-2} \text{d}^{-1}$ at stations Bel-11 and Bel-13, respectively; Fig. 3c, d, and Tables S1 and S2). Although N_2
306 fixation was not detected in the central Bay of Biscay (stations Bel-3 and Bel-5), rates recorded at all the other sites
307 were relatively high, not only in shelf-influenced areas (141 and 262 $\mu\text{mol N m}^{-2} \text{d}^{-1}$ at stations Geo-1 and Geo-2,
308 respectively) but also in the open ocean (average activities between 81–384 $\mu\text{mol N m}^{-2} \text{d}^{-1}$ at stations Bel-7, Bel-9,
309 Geo-13 and Geo-21).

310 By fuelling the bioavailable nitrogen pool, N_2 fixation may support marine primary production (PP), but the extent of
311 this contribution needs to be established for areas outside tropical and subtropical regions. PP rates measured here are
312 of similar range if not slightly higher than those reported in earlier works for subtropical to temperate waters of the
313 northeast Atlantic (32 to 137 $\text{mmol C m}^{-2} \text{d}^{-1}$ relative to 19 to 103 $\text{mmol C m}^{-2} \text{d}^{-1}$) (Marañón et al., 2000; Fernández
314 et al., 2005; Poulton et al., 2006; Fonseca-Batista et al., 2017). However, N_2 fixation contributions to PP in the
315 present work (1–28% of PP) reached values twice as high as those reported in other studies for the tropical and
316 subtropical northeast Atlantic (contributions to PP ranging from < 1% to 12%) (Voss et al., 2004; Rijkenberg et al.,
317 2011; Fonseca-Batista et al., 2017). This observation further questions the general idea that oligotrophic surface
318 waters of tropical and subtropical regions are the key environment where marine primary productivity is significantly
319 supported by diazotrophic activity (Capone et al., 2005; Luo et al., 2014). Nevertheless, it is important to keep in
320 mind that our computation relies on the assumption that only photoautotrophic diazotrophs contribute to bulk N_2
321 fixation, which is not always the case, particularly in the present study, where mostly heterotrophic diazotrophs were

322 observed. However, it is likely that all the recently fixed-nitrogen ultimately becomes available for the whole marine
323 autotrophic community.

324 Previous studies in the open waters of the Iberian Basin (35–50° N, east of 25° W) reported relatively lower N₂
325 fixation rates (from < 0.1 to 140 μmol N m⁻² d⁻¹), regardless of whether the bubble-addition method (Montoya et al.,
326 1996) or the dissolution method (Mohr et al., 2010; Großkopf et al., 2012) were used. However, these studies were
327 carried out largely outside the bloom period, either during the late growth season (summer and autumn) (Moore et al.,
328 2009; Benavides et al., 2011; Snow et al., 2015; Riou et al., 2016; Fonseca-Batista et al., 2017) or during winter
329 (Rijkenberg et al., 2011; Agawin et al., 2014). In contrast, the present study took place in spring, during or just at the
330 end of the vernal phytoplankton bloom. Differences in timing of these various studies and to a lesser extent, different
331 methodologies (bubble-addition versus dissolution method) may explain the discrepancies in diazotrophic activity
332 observed between our study and earlier works. Yet, the 20 months survey by Moreira-Coello et al. (2017) in nitrogen-
333 rich temperate coastal waters in the southern Bay of Biscay, covering the seasonal spring bloom and upwelling
334 pulses, did not revealed significant N₂ fixation activities: from 0.1 to 1.6 μmol N m⁻² d⁻¹ (up to 3 orders of magnitude
335 lower than those reported here). However, unlike our study, this work was carried out not only using the bubble-
336 addition method but also in an inner coastal system, as opposed to the mainly open waters studied here, making it
337 difficult to predict which variable or combination of variables caused the difference in observations between both
338 studies.

339 Our maximal values recorded at stations Bel-11 and Bel-13 are one order of magnitude higher than maximal N₂
340 fixation rates reported further south for the eastern tropical and subtropical North Atlantic (reaching up to 360–424
341 μmol N m⁻² d⁻¹) (Großkopf et al., 2012; Subramaniam et al., 2013; Fonseca-Batista et al., 2017). Besides these two
342 highly active sites, N₂ fixation rates at the other studied locations (ranging between 81–384 μmol N m⁻² d⁻¹) were still
343 in the upper range of values reported for the whole eastern Atlantic region. Yet, conditions favouring N₂ fixation are
344 commonly believed to be met in tropical and subtropical regions where highest activities have mostly been measured,
345 particularly in the eastern North Atlantic (e.g., higher seawater temperature, DIN limiting concentrations, excess
346 phosphorus supply through eastern boundary upwelling systems) (Capone et al., 2005; Deutsch et al., 2007; Luo et
347 al., 2014; Fonseca-Batista et al., 2017).

348 In the Atlantic Ocean, very high N₂ fixation rates up to ~1000 μmol N m⁻² d⁻¹ as observed here, have only been
349 reported for temperate coastal waters of the Northwest Atlantic (up to 838 μmol N m⁻² d⁻¹) (Mulholland et al., 2012)
350 and for tropical shelf-influenced and mesohaline waters of the Caribbean and Amazon River plume (maximal rates
351 ranging between 898 and 1600 μmol N m⁻² d⁻¹) (Capone et al., 2005; Montoya et al., 2007; Subramaniam et al.,
352 2008). Shelf and mesohaline areas have indeed been shown to harbour considerable N₂ fixation activity, not only in
353 tropical regions (Montoya et al., 2007; Subramaniam et al. 2008) but also in areas from temperate to polar regions
354 (Rees et al., 2009; Blais et al., 2012; Mulholland et al., 2012; Shiozaki et al., 2015). Yet, the environmental
355 conditions that lead to the high N₂ fixation rates in those regions are currently not well understood. For tropical
356 mesohaline systems the conditions proposed to drive such an intense diazotrophic activity include the occurrence of
357 highly competitive diatom-diazotrophs associations and the influence of excess phosphorus input (i.e., excess relative
358 to the canonical Redfield P/N ratio; expressed as P*) from the Amazon River (Subramaniam et al., 2008). However,
359 such conditions of excess P were not observed in previous studies carried out in high latitude shelf regions with
360 elevated N₂ fixation activities (Blais et al., 2012; Mulholland et al., 2012; Shiozaki et al., 2015), nor was it distinctly
361 apparent in the present study (see section 4.3). In addition, while tropical mesohaline regions are characterized by the
362 predominance of diatom-diazotroph associations (and filamentous *Trichodesmium* spp.), in temperate shelf areas the
363 diazotrophic community is reported to be essentially dominated by UCYN-A and heterotrophic bacteria (Rees et al.,

364 2009; Blais et al., 2012; Mulholland et al., 2012; Agawin et al., 2014; Shiozaki et al., 2015; Moreira-Coello et al.,
365 2017).

366

367 **4.2 Features of the diazotrophic community composition in the temperate North Atlantic**

368 Our qualitative assessment of *nifH* diversity revealed a predominance of UCYN-A symbionts, only at the two stations
369 with highest recorded surface N₂ fixation rates (up to 65.4 and 45.0 nmol N L⁻¹ d⁻¹ at Bel-11 and Bel-13, respectively;
370 Table S1) while the remaining *nifH* sequences recovered belonged to heterotrophic diazotrophs, at Bel-13 and also at
371 all the other sites where *nifH* genes could be detected. No *Trichodesmium nifH* sequences were recovered from either
372 BG2014/14 or GEOVIDE DNA samples, and the absence of the filamentous cyanobacteria was also confirmed by a
373 CHEMTAX analysis of phytoplankton pigments (M. Tonnard, personal communication, January 2018). Previous
374 work in temperate regions of the global ocean, including the Iberian Margin also reported that highest N₂ fixation
375 activities were predominantly related to the presence of UCYN-A symbionts, followed by heterotrophic bacteria,
376 while *Trichodesmium* filaments were low or undetectable (Needoba et al., 2007; Rees et al., 2009; Mulholland et al.,
377 2012; Agawin et al., 2014; Shiozaki et al., 2015; Moreira-Coello et al., 2017).

378 UCYN-A (in particular from the UCYN-A1 clade) were shown to live in symbioses with single-celled
379 prymnesiophyte algae (Thompson et al., 2012). This symbiotic association, considered obligate, has been reported to
380 be particularly abundant in the central and eastern basin of the North Atlantic (Rees et al., 2009; Krupke et al., 2014;
381 Cabello et al., 2015; Martínez-Pérez et al., 2016).

382 Besides UCYN-A, all the remaining *nifH* sequences recovered from both cruises, although obtained through different
383 approaches, belonged to non-cyanobacterial diazotrophs. The phylogenetic tree (Fig. 6) showed that the non-
384 cyanobacterial diazotrophs clustered with (1) Verrucomicrobia, a phylum yet poorly known that includes aerobic to
385 microaerophile methanotrophs groups, found in a variety of environments (Khadem et al., 2010; Wertz et al., 2012),
386 (2) anaerobic bacteria, obligate or facultative, mostly affiliated to Cluster III phylotypes of functional nitrogenase
387 (e.g., Bacteroidetes, Firmicutes, Proteobacteria) and finally (3) phylotypes from Clusters I, II, and IV (e.g.,
388 Proteobacteria and Firmicutes). Among the Cluster III phylotypes, Bacteroidetes are commonly encountered in the
389 marine environment, and are known as specialized degraders of organic matter that preferably grow attached to
390 particles or algal cells (Fernández-Gómez et al., 2013). N₂ fixation activity has previously been reported in five
391 Bacteroidetes strains including *Bacteroides graminisolvens*, *Paludibacter propionicigenes* and *Dysgonomonas gadei*
392 (Inoue et al., 2015) which are the closest cultured relatives of the *nifH*-OTUs detected at station Bel-13 (Fig. 6).
393 Anaerobic Cluster III phylotypes have been previously recovered from different ocean basins (Church et al., 2005;
394 Langlois et al., 2005, 2008; Man-Aharonovich et al., 2007; Rees et al., 2009; Halm et al., 2012; Mulholland et al.,
395 2012). These diazotrophs were suggested to benefit from anoxic microzones found within marine snow particles or
396 zooplankton guts to fix N₂ thereby avoiding oxygenic inhibition of their nitrogenase enzyme (Braun et al., 1999;
397 Church et al., 2005; Scavotto et al., 2015). Therefore, the bloom to early post-bloom conditions, prevailing during our
398 study, were likely beneficial to the development of diazotrophic groups that depend on the availability of detrital
399 organic matter or the association with grazing zooplankton. In contrast, at the northern most Geo-21 station, we
400 observed a dominance of Gammaproteobacteria phylotypes belonging to a recently identified clade of marine
401 diazotrophs within the Oceanospirillales (Delmont et al., 2018).

402 These observations tend to strengthen the idea of a substantial role played not only by UCYN-A (Cabello et al., 2015;
403 Martínez-Pérez et al., 2016) but also by non-cyanobacteria (Halm et al., 2012; Shiozaki et al., 2014; Langlois et al.,
404 2015) in oceanic N₂ fixation. Although it is possible to assign a broad taxonomic affiliation to classify the *nifH* genes,

405 we know very little with respect to their physiology, their role in the ecosystem and the factors that control their
406 distribution largely due to the lack of representative whole genome sequences and environmentally relevant strains
407 available for experimentation (Bombar et al., 2016). While studies have been reporting on the widespread distribution
408 of UCYN-A and heterotrophic diazotrophs, their contribution to in situ activity remains until now poorly quantified.
409

410 **4.3 Key environmental drivers of N₂ fixation**

411 Environmental conditions that promote autotrophic and heterotrophic N₂ fixation activity in the ocean are currently
412 not well understood (Luo et al., 2014). While heterotrophic diazotrophs would not be directly affected by the
413 commonly recognized environmental controls of autotrophic diazotrophy such as solar radiation, seawater
414 temperature and DIN, as they possess fundamentally different ecologies, the molecular and cellular processes for
415 sustaining N₂ fixation activity would nevertheless require a supply of dFe and P (Raven, 1988; Howard & Rees,
416 1996; Mills et al., 2004; Snow et al., 2015). Besides the need for these critical inorganic nutrients, heterotrophic N₂
417 fixation was also recently shown to be highly dependent on the availability of organic matter (Bonnet et al., 2013;
418 Rahav et al., 2013, 2016; Loescher et al., 2014).

419 Findings from the GEOVIDE cruise tend to support the hypothesis of a stimulating effect of organic matter
420 availability on N₂ fixation activity at the time of our study. Lemaitre et al. (2018) report that the upper 100–120 m
421 waters of the Iberian Basin (stations Geo-1 and Geo-13) and the West European Basin (Geo-21) carried significant
422 particulate organic carbon loads (POC of 166, 171 and 411 mmol C m⁻², respectively) with a dominant fraction of
423 small size POC (1–53 μm; 75%, 92% and 64% of total POC, respectively). Smaller cells, usually being slow-sinking
424 particles, are more easily remineralized in surface waters (Villa-Alfageme et al., 2016). This is confirmed by the very
425 low export efficiency observed at stations Geo-13 and Geo-21, evidencing an efficient shallow remineralisation (only
426 3 to 4% of euphotic layer integrated PP reaching the depth of export at these stations; (Lemaitre et al., 2018). This
427 availability of organic matter in the upper layers likely contributed to supplying remineralized P (organic P being
428 generally more labile than other organic nutrients; Vidal et al., 1999, 2003) and to enhancing the residence time of
429 dFe originating from atmospheric deposition due to the formation of organic ligands (Jickells, 1999; de Baar and de
430 Jong, 2001; Sarthou et al., 2003).

431 P* values from the BG2014/14 cruise (Table S1) and the climatological P* data for the Iberian Basin (Garcia et al.,
432 2013) do not exhibit a clear PO₄³⁻ excess in the region (P* ranging between -0.1 and 0.1 μmol L⁻¹; Fig. 1 and Tables
433 S1 and S2). Nevertheless, Spearman rank correlations indicate that volumetric N₂ fixation rates were significantly
434 correlated with the BG2014/14 shipboard P* values (n = 24, p < 0.01, Table S4), with stations Bel-11 and Bel-13
435 weighing heavily in this correlation. Without the data from these two sites (data not shown) the correlation between
436 in situ P* and N₂ fixation rates is no longer significant (n = 16, p = 0.163), with P* becoming highly correlated with
437 PP and Chl *a* (n = 16, p = 0.0257 and 0.016, respectively). This suggests that P* effect on N₂ fixation, although not
438 clearly evident from absolute values, was most important at stations Bel-11 and Bel-13 but nonetheless existent at the
439 other sites (Bel-7 and Bel-9). The impact of weak P* values in oligotrophic waters depleted in DIN and PO₄³⁻ but
440 replete in dFe might in fact reflect the direct use of dissolved organic phosphorus (DOP). Indeed, according to
441 Landolfi et al. (2015) diazotrophy ensures the supply of additional N and energy for the enzymatic mineralization of
442 DOP (synthesis of extracellular alkaline phosphatase). Therefore, a likely enhanced DOP release towards the end of
443 the spring bloom may have contributed to sustaining N₂ fixation in the studied region. Such DOP utilization has
444 indeed been reported for various marine organisms, particularly diazotrophic cyanobacteria (Dyhrman et al., 2006;
445 Dyhrman & Haley, 2006) and bacterial communities (Luo et al., 2009).

446 Supply routes of dFe to the surface waters of the investigated area relied on lateral advection from the continental
447 shelf (stations Geo-1 and Geo-2) (Tonnard et al., 2018), vertical mixing due to post-winter convection (Thuróczy et
448 al., 2010; Rijkenberg et al., 2012; García-Ibáñez et al., 2015), and/or atmospheric dust deposition (dry + wet). In the
449 following we discuss that atmospheric deposition may have been particularly important for the area of stations Bel-11
450 and Bel-13 receiving warm and saline surface waters from the subtropics.

451 Atmospheric aerosol deposition determined during the GEOVIDE cruise (Shelley et al., 2017) as well as the satellite-
452 based dust deposition (dry + wet) averaged over the month of May 2014 (Fig. S3b; Giovanni online satellite data
453 system, NASA Goddard Earth Sciences Data and Information Services Center) reveal rather weak dust loadings over
454 the investigated region, resulting in areal N₂ fixation rates being actually inversely correlated to the satellite-based
455 average dust input ($p < 0.01$, Table S3). In contrast, satellite-based dust deposition (dry + wet) averaged over the
456 month of April 2014 (i.e. preceding the timing of sampling) indicate high values over the subtropical waters located
457 south of the studied region (Fig. S3a;). The θ/S diagrams at stations Bel-11 and Bel-13 (and to a lesser extent at Geo-
458 13; Fig. S1) illustrate the presence of very warm and saline waters and satellite SST images suggest these were
459 advected from the subtropics (Fig. S2). We thus argue that advection of surface waters from south of the study area
460 represented a source of atmospherically derived dFe and contributed to driving the high N₂ fixation activity recorded
461 at stations Bel-11 and Bel-13. This resulted in N₂ fixation rates there being positively (although weakly) correlated (p
462 = 0.45, Table S3) with the April average dust input.

463 For the central Bay of Biscay, where N₂ fixation was below detection limit (stations Bel-3 and Bel-5), dust deposition
464 in April 2014 was also the lowest, suggesting that N₂ fixation there might have been limited by dFe availability.
465 Indeed, at stations Bel-3 and Bel-5 diazotrophic activity in surface waters was boosted following dFe amendments ($>$
466 25 nmol N L⁻¹ d⁻¹; Li et al., 2018).

467 Thus, the enhanced N₂ fixation activity at stations Bel-11 and Bel-13, as compared to the other sites, was likely
468 stimulated by the combined effects of the presence of highly competitive prymnesiophyte-UCYN-A symbionts,
469 organic matter as a source of DOP, positive P* signatures, and advection of subtropical surface waters enriched in
470 dFe.

471 These statements are further supported by the outcome of a multivariate statistical analysis providing a
472 comprehensive view of the environmental features influencing N₂ fixation. A principal component analysis (PCA;
473 Fig. 7 and Tables S2 and S5) generated two components (or axes) explaining 68% of the system's variability. Axis 1
474 illustrates the productivity of the system, or more precisely the oligotrophic state towards which it was evolving. Axis
475 1 is defined by a strong positive relation with surface temperature (reflecting the onset of stratification, particularly
476 for stations Bel-11 and Bel-13; Fig. 7) and an inverse relation with PP and associated variables (Chl *a*, NH₄⁺, NO₃⁻ +
477 NO₂⁻), which reflects the prevailing post-bloom conditions of the system. Sites characterized by a moderate (Bel-3
478 and Bel-5) to high (Bel-7, Geo-21 and to a lesser extent Geo-13) PP appear indeed tightly linked to these PP-
479 associated variables as illustrated in Fig. 7. Axis 2 is defined by the positive relation with surface salinity and P* (Fig.
480 7) and reflects the advection of surface waters of subtropical origin, for stations Bel-11, Bel-13 and Geo-13. For
481 stations Geo-1 and Geo-2, the inverse relation with surface salinity (Fig. 7) is interpreted to reflect fluvial inputs
482 (Tonnard et al., 2018). Finally, this statistical analysis indicates that N₂ fixation activity was likely influenced by the
483 two PCA components, tentatively identified as productivity (axis 1) and surface water advection (axis 2) from the
484 shelf and the subtropical region.

485 5 Conclusions

486 The present work highlights the occurrence of elevated N₂ fixation activities (81–1533 μmol N m⁻² d⁻¹) in spring 2014
487 in open waters of the temperate eastern North Atlantic, off the Iberian Peninsula. These rates exceed those reported
488 by others for the Iberian Basin, but which were largely obtained outside the bloom period (from < 0.1 to 140 μmol N
489 m⁻² d⁻¹). In contrast we did not detect any N₂ fixation activity in the central Bay of Biscay. At sites where significant
490 N₂ fixation activity was detected, rates were similar to or up to an order of magnitude larger compared to values for
491 the eastern tropical and subtropical North Atlantic, regions commonly believed to represent the main harbour of
492 oceanic N₂ fixation for the eastern Atlantic. Assuming that the carbon vs nitrogen requirements by these N₂ fixers
493 obey the Redfield stoichiometry, N₂ fixation was found able to contribute 1–3% of the euphotic layer daily PP and
494 even up to 23–25% at the sites where N₂ fixation activity was highest. The Pymnesiophyte-symbiont *Candidatus*
495 *Atelocyanobacterium thalassa* (UCYN-A) contributed most to the *nifH* sequences recovered at the two sites where N₂
496 fixation activity was highest, while the remaining sequences belonged exclusively to heterotrophic bacteria. We
497 support that the unexpectedly high N₂ fixation activity recorded at the time of our study was sustained by (i) organic
498 matter availability in these open waters, resulting from the prevailing vernal bloom to post-bloom conditions, in
499 combination with (ii) excess phosphorus signatures which appeared to be tightly related to diazotrophic activity
500 particularly at the two most active sites. Yet these observations and hypotheses rely on the availability of dFe with
501 evidence for input from shelf waters and pulsed atmospheric dust deposition being a significant source of iron.
502 Further studies are required to investigate this possible link between N₂ fixation activity and phytoplankton bloom
503 under iron-replete conditions in the studied region and similar areas, as these would require to be considered in future
504 assessment of global N₂ fixation.

505

506

507 Data availability. The data associated with the paper are available from the corresponding author upon request.

508

509 The Supplement related to this article is available.

510

511 Competing interests. The authors declare that they have no conflict of interest.

512

513

514 *Acknowledgements.* We thank the Captains and the crews of R/V *Belgica* and R/V *Pourquoi pas?* for their skilful
515 logistic support. A very special thank goes to the chief scientists G. Sarthou and P. Lherminier of the GEOVIDE
516 expedition for the great work experience and wonderful support on board. We would like to give special thanks to
517 Pierre Branellec, Michel Hamon, Catherine Kermabon, Philippe Le Bot, Stéphane Leizour, Olivier Ménage
518 (Laboratoire d'Océanographie Physique et Spatiale), Fabien Pérault and Emmanuel de Saint Léger (Division
519 Technique de l'INSU, Plouzané, France) for their technical expertise during clean CTD deployments. We thank A.
520 Roukaerts and D. Verstraeten for their assistance with laboratory analyses at the Vrije Universiteit Brussel. We
521 acknowledge Ryan Barkhouse for the collection of the DNA samples during the GEOVIDE cruise, Jennifer Tolman
522 and Jenni-Marie Ratten for the *nifH* amplification and Tag sequencing. P. Lherminier, P. Tréguer, E. Grossteffan, and
523 M. Le Goff are gratefully acknowledged for providing us with the shipboard physico-chemical data including CTD
524 and nitrate plus nitrite data from the GEOVIDE expedition. Shiptime for the *Belgica* BG2014/14 cruise was granted
525 by Operational Directorate 'Natural Environment' (OD Nature) of the Royal Institute of Natural Sciences, Belgium.
526 OD Nature (Ostend) is also acknowledged for their assistance in CTD operations and data acquisition on board the

527 R/V *Belgica*. This work was financed by Flanders Research Foundation (FWO contract G0715.12N) and Vrije
528 Universiteit Brussel, R&D, Strategic Research Plan "Tracers of Past & Present Global Changes". Additional funding
529 was provided by the Fund for Scientific Research - FNRS (F.R.S.-FNRS) of the Wallonia-Brussels Federation
530 (convention no. J.0150.15). X. Li was a FNRS doctorate Aspirant fellow (mandate no. FC99216). This study was also
531 supported, through the GEOVIDE expedition, by the French National Research Agency (ANR-13-B506-0014), the
532 Institut National des Sciences de L'Univers (INSU) of the Centre National de la Recherche Scientifique (CNRS), and
533 the French Institute for Marine Science (Ifremer). This work was logistically supported for the by DT-INSU and
534 GENAVIR. Finally, this work is also a contribution to the Labex OT-Med [ANR-11-LABEX-0061, www.otmed.fr]
535 funded by the « Investissements d'Avenir », French Government project of the French National Research Agency
536 [ANR, www.agence-nationale-recherche.fr] through the A*Midex project [ANR-11-IDEX-0001-02], funding V.
537 Riou during the preparation of the manuscript.

538 **References**

- 539 Agawin, N. S. R., Benavides, M., Busquets, A., Ferriol, P., Stal, L. J. and Arístegui, J.: Dominance of unicellular
540 cyanobacteria in the diazotrophic community in the Atlantic Ocean, *Limnol. Oceanogr.*, 59(2), 623–637,
541 doi:10.4319/lo.2014.59.2.0623, 2014.
- 542 Ambar, I. and Fiúza, A. F. G.: Some features of the Portugal Current System: a poleward slope undercurrent, an
543 upwelling-related summer southward flow and an autumn-winter poleward coastal surface current, in: Proceedings
544 of the Second International Conference on Air-Sea Interaction and on Meteorology and Oceanography of the
545 Coastal Zone, edited by: Katsaros, K. B., Fiúza, A. F. G. and Ambar, I., American Meteorological Society, Boston,
546 Massachusetts, United States, 286-287, 1994.
- 547 Benavides, M., Agawin, N., Arístegui, J., Ferriol, P. and Stal, L.: Nitrogen fixation by *Trichodesmium* and small
548 diazotrophs in the subtropical northeast Atlantic, *Aquat. Microb. Ecol.*, 65(1), 43–53, doi:10.3354/ame01534,
549 2011.
- 550 Blais, M., Tremblay, J.-É., Jungblut, A. D., Gagnon, J., Martin, J., Thaler, M. and Lovejoy, C.: Nitrogen fixation and
551 identification of potential diazotrophs in the Canadian Arctic, *Global Biogeochem. Cycles*, 26(3), 1–13,
552 doi:10.1029/2011GB004096, 2012.
- 553 Bombar, D., Paerl, R. W. and Riemann, L.: Marine Non-Cyanobacterial Diazotrophs: Moving beyond Molecular
554 Detection, *Trends Microbiol.*, 24(11), 916–927, doi:10.1016/j.tim.2016.07.002, 2016.
- 555 Bonnet, S., Dekaezemacker, J., Turk-Kubo, K. A., Moutin, T., Hamersley, R. M., Grosso, O., Zehr, J. P. and Capone,
556 D. G.: Aphotic N₂ fixation in the Eastern Tropical South Pacific Ocean., *PLoS One*, 8(12), e81265,
557 doi:10.1371/journal.pone.0081265, 2013.
- 558 Braun, S. T., Proctor, L. M., Zani, S., Mellon, M. T. and Zehr, J. P. Y.: Molecular evidence for zooplankton-
559 associated nitrogen-fixing anaerobes based on amplification of the *nifH* gene, *FEMS Microbiol. Ecol.*, 28, 273–
560 279, 1999.
- 561 Breitbarth, E., Oschlies, A. and LaRoche, J.: Physiological constraints on the global distribution of *Trichodesmium* –
562 effect of temperature on diazotrophy, *Biogeosciences*, 4, 53–61, doi:10.5194/bg-4-53-2007, 2007.
- 563 Cabello, A. M., Cornejo-Castillo, F. M., Raho, N., Blasco, D., Vidal, M., Audic, S., de Vargas, C., Latasa, M.,
564 Acinas, S. G. and Massana, R.: Global distribution and vertical patterns of a prymnesiophyte–cyanobacteria
565 obligate symbiosis, *ISME J.*, 1–14, doi:10.1038/ismej.2015.147, 2015.

566 Capone, D. G.: Trichodesmium, a Globally Significant Marine Cyanobacterium, *Science*, 276(5316), 1221–1229,
567 doi:10.1126/science.276.5316.1221, 1997.

568 Capone, D. G., Burns, J. A., Montoya, J. P., Subramaniam, A., Mahaffey, C., Gunderson, T., Michaels, A. F. and
569 Carpenter, E. J.: Nitrogen fixation by Trichodesmium spp.: An important source of new nitrogen to the tropical and
570 subtropical North Atlantic Ocean, *Global Biogeochem. Cycles*, 19(2), 1–17, doi:10.1029/2004GB002331, 2005.

571 Caporaso, J. G., Kuczynski, J., Stombaugh, J., Bittinger, K., Bushman, F. D., Costello, E. K., Fierer, N., Peña, A. G.,
572 Goodrich, J. K., Gordon, J. I., Huttley, G. a, Kelley, S. T., Knights, D., Koenig, J. E., Ley, R. E., Lozupone, C. a,
573 Mcdonald, D., Muegge, B. D., Pirrung, M., Reeder, J., Sevinsky, J. R., Turnbaugh, P. J., Walters, W. a, Widmann,
574 J., Yatsunencko, T., Zaneveld, J. and Knight, R.: QIIME allows analysis of high- throughput community sequencing
575 data Intensity normalization improves color calling in SOLiD sequencing, *Nat. Publ. Gr.*, 7(5), 335–336,
576 doi:10.1038/nmeth0510-335, 2010.

577 Church, M. J., Jenkins, B. D., Karl, D. M. and Zehr, J. P.: Vertical distributions of nitrogen-fixing phylotypes at Stn
578 ALOHA in the oligotrophic North Pacific Ocean, *Aquat. Microb. Ecol.*, 38(1), 3–14, doi:10.3354/ame038003,
579 2005.

580 Comeau, A. M., Douglas, G. M. and Langille, M. G. I.: Microbiome Helper: a Custom and Streamlined Workflow for
581 Microbiome Research, *mSystems*, 2(1), e00127-16, doi:10.1128/mSystems.00127-16, 2017.

582 de Boyer Montégut, C., Madec, G., Fischer, A. S., Lazar, A., and Iudicone, D.: Mixed layer depth over the global
583 ocean: An examination of profile data and a profile-based climatology. *J. Geophys. Res.*, 109(12), 1–20.
584 <https://doi.org/10.1029/2004JC002378>, 2004.

585 Delmont, T. O., Quince, C., Shaiber, A., Esen, Ö. C., Lee, S. T., Rappé, M. S., McLellan, S. L., Lückner, S. and Eren,
586 A. M.: Nitrogen-fixing populations of Planctomycetes and Proteobacteria are abundant in surface ocean
587 metagenomes, *Nat. Microbiol.*, 3(8), 804–813, doi:10.1038/s41564-018-0209-4, 2018.

588 Deutsch, C., Sarmiento, J. L., Sigman, D. M., Gruber, N. and Dunne, J. P.: Spatial coupling of nitrogen inputs and
589 losses in the ocean., *Nature*, 445(7124), 163–167, doi:10.1038/nature05392, 2007.

590 Dore, J. E., Brum, J. R., Tupas, L. and Karl, D. M.: Seasonal and interannual variability in sources of nitrogen
591 supporting export in the oligotrophic subtropical North Pacific Ocean, *Limnol. Ocean.*, 47(6), 1595–1607, 2002.

592 Dyhrman, S. T. and Haley, S. T.: Phosphorus scavenging in the unicellular marine diazotroph *Crocospaera watsonii*
593 phosphorus scavenging in the unicellular marine diazotroph *Crocospaera watsonii*, *Appl. Environ. Microbiol.*,
594 72(2), 1452–1458, doi:10.1128/AEM.72.2.1452, 2006.

595 Dyhrman, S. T., Chappell, P. D., Haley, S. T., Moffett, J. W., Orchard, E. D., Waterbury, J. B. and Webb, E. A.:
596 Phosphonate utilization by the globally important marine diazotroph Trichodesmium, *Nature*, 439(7072), 68–71,
597 doi:10.1038/nature04203, 2006.

598 Falkowski, P. G.: Evolution of the nitrogen cycle and its influence on the biological sequestration of CO₂ in the
599 ocean, *Nature*, 387(6630), 272–275, doi:10.1038/387272a0, 1997.

600 Farnelid, H., Andersson, A. F., Bertilsson, S., Al-Soud, W. A., Hansen, L. H., Sørensen, S., Steward, G. F.,
601 Hagström, Å. and Riemann, L.: Nitrogenase gene amplicons from global marine surface waters are dominated by
602 genes of non-cyanobacteria, *PLoS One*, 6(4), doi:10.1371/journal.pone.0019223, 2011.

603 Farnelid, H., Bentzon-Tilia, M., Andersson, A. F., Bertilsson, S., Jost, G., Labrenz, M., Jürgens, K. and Riemann, L.:
604 Active nitrogen-fixing heterotrophic bacteria at and below the chemocline of the central Baltic Sea., *ISME J.*, 7(7),
605 1413–23, doi:10.1038/ismej.2013.26, 2013.

606 Fernández-Gómez, B., Richter M, Schüler M, Pinhassi, J., Acinas, S., González, J. and Pedrós-Alió, C.: Ecology of
607 marine Bacteroidetes: a comparative genomics approach, *ISME J.*, 7(5), 1026–1037, doi:10.1038/ismej.2012.169,
608 2013.

609 Fernández, A., Mouriño-Carballido, B., Bode, A., Varela, M. and Marañón, E.: Latitudinal distribution of
610 *Trichodesmium* spp. and N₂ fixation in the Atlantic Ocean, *Biogeosciences*, 7(2), 3167–3176, doi:10.5194/bg-7-
611 3167-2010, 2010.

612 Fernández I., C., Raimbault, P., Garcia, N. and Rimmelin, P.: An estimation of annual new production and carbon
613 fluxes in the northeast Atlantic Ocean during 2001, *J. Geophys. Res.*, 110(C7), 1–15, doi:10.1029/2004JC002616,
614 2005.

615 Fiúza, A.F.G.: Hidrologia e dinâmica das águas costeiras de Portugal (Hydrology and dynamics of the Portuguese
616 coastal waters), Ph.D. thesis, Universidade de Lisboa, Portugal, 294 pp., 1984.

617 Fonseca-Batista, D., Dehairs, F., Riou, V., Fripiat, F., Elskens, M., Deman, F., Brion, N., Quéroué, F., Bode, M. and
618 Auel, H.: Nitrogen fixation in the eastern Atlantic reaches similar levels in the Southern and Northern Hemisphere,
619 *J. Geophys. Res. Ocean.*, 122, 4618–4632, doi:10.1002/2016JC012335, 2017.

620 Foster, R. A., Subramaniam, A., Mahaffey, C., Carpenter, E. J., Capone, D. G. and Zehr, J. P.: Influence of the
621 Amazon River plume on distributions of free-living and symbiotic cyanobacteria in the western tropical north
622 Atlantic Ocean, *Limnol. Oceanogr.*, 52(2), 517–532, doi:10.4319/lo.2007.52.2.0517, 2007.

623 Frouin, R., Fiúza, A. F. G., Ambar, I. and Boyd, T. J.: Observations of a poleward surface current off the coasts of
624 Portugal and Spain during winter, *J. Geophys. Res.*, 95(C1), 679, doi:10.1029/JC095iC01p00679, 1990.

625 García-Ibáñez, M. I., Pardo, P. C., Carracedo, L. I., Mercier, H., Lherminier, P., Ríos, A. F. and Pérez, F. F.:
626 Structure, transports and transformations of the water masses in the Atlantic Subpolar Gyre, *Prog. Oceanogr.*, 135,
627 18–36, doi:10.1016/j.pocean.2015.03.009, 2015.

628 Garcia, H. E., Locarnini, R. A., Boyer, T. P., Antonov, J. I., Baranova, O. K., Zweng, M. M., Reagan, J. R. and
629 Johnson, D. R.: *World Ocean Atlas 2013, Volume 4 : Dissolved Inorganic Nutrients (phosphate, nitrate, silicate)*,
630 Silver Spring, Maryland, USA., 2013.

631 Grasshoff, K., Ehrhardt, M. and Kremling, K.: *Methods of Seawater Analysis. Second, Revised and Extended*
632 *Edition*, Verlag Chemie GmbH, D-6940 Weinheim, Germany., 1983.

633 Großkopf, T., Mohr, W., Baustian, T., Schunck, H., Gill, D., Kuypers, M. M. M., Lavik, G., Schmitz, R. A., Wallace,
634 D. W. R. and LaRoche, J.: Doubling of marine dinitrogen-fixation rates based on direct measurements, *Nature*,
635 488(7411), 361–364, doi:10.1038/nature11338, 2012.

636 Gruber, N.: The Marine Nitrogen Cycle: Overview and Challenges, in: *Nitrogen in the Marine Environment*, edited
637 by: Capone, D. G., Bronk, D. A., Mulholland, M. M., Carpenter E. J., Academic Press, Cambridge, Massachusetts,
638 United States, 1–50, <https://doi.org/10.1016/B978-0-12-372522-6.X0001-1>, 2008.

639 Halm, H., Lam, P., Ferdelman, T. G., Lavik, G., Dittmar, T., LaRoche, J., D’Hondt, S. and Kuypers, M. M. M.:
640 Heterotrophic organisms dominate nitrogen fixation in the South Pacific Gyre., *ISME J.*, 6(6), 1238–49,
641 doi:10.1038/ismej.2011.182, 2012.

642 Hama, T., Miyazaki, T., Ogawa, Y., Iwakuma, T., Takahashi, M., Otsuki, A. and Ichimura, S.: Measurement of
643 photosynthetic production of a marine phytoplankton population using a stable ¹³C isotope, *Mar. Biol.*, 73, 31–36,
644 1983.

645 Holmes, R. M., Aminot, A., Kérouel, R., Hooker, B. A. and Peterson, B. J.: A simple and precise method for
646 measuring ammonium in marine and freshwater ecosystems, *Can. J. Fish. Aquat. Sci.*, 56(10), 1801–1808,
647 doi:10.1139/f99-128, 1999.

648 Howard, J. B. and Rees, D. C.: Structural Basis of Biological Nitrogen Fixation., *Chem. Rev.*, 96(7), 2965–2982,
649 doi:10.1021/cr9500545, 1996.

650 Inoue, J., Oshima, K., Suda, W., Sakamoto, M., Iino, T., Noda, S., Hongoh, Y., Hattori, M. and Ohkuma, M.:
651 Distribution and evolution of nitrogen fixation genes in the phylum Bacteroidetes., *Microbes Environ.*, 30(1), 44–
652 50, doi:10.1264/jsme2.ME14142, 2015.

653 Jickells, T. D.: The inputs of dust derived elements to the Sargasso Sea; a synthesis, *Mar. Chem.*, 68(1–2), 5–14,
654 doi:10.1016/S0304-4203(99)00061-4, 1999.

655 Khadem, A. F., Pol, A., Jetten, M. S. M. and Op Den Camp, H. J. M.: Nitrogen fixation by the verrucomicrobial
656 methanotroph “*Methylacidiphilum fumariolicum*” SolV, *Microbiology*, 156(4), 1052–1059,
657 doi:10.1099/mic.0.036061-0, 2010.

658 Kimura, M.: A simple method for estimating evolutionary rates of base substitutions through comparative studies of
659 nucleotide sequences, *J. Mol. Evol.*, 16(2), 111–120, doi:10.1007/BF01731581, 1980.

660 Krupke, A., Lavik, G., Halm, H., Fuchs, B. M., Amann, R. I. and Kuypers, M. M. M.: Distribution of a consortium
661 between unicellular algae and the N₂ fixing cyanobacterium UCYN-A in the North Atlantic Ocean, *Environ.*
662 *Microbiol.*, 16(10), 3153–3167, doi:10.1111/1462-2920.12431, 2014.

663 Kumar, S., Stecher, G. and Tamura, K.: MEGA7: Molecular Evolutionary Genetics Analysis version 7.0 for bigger
664 datasets., *Mol. Biol. Evol.*, msw054, doi:10.1093/molbev/msw054, 2016.

665 Landolfi, A., Koeve, W., Dietze, H., Kähler, P. and Oschlies, A.: A new perspective on environmental controls,
666 *Geophys. Res. Lett.*, 42(May), 4482–2289, doi.org/10.1002/2015GL063756, 2015.

667 Langlois, R., Großkopf, T., Mills, M., Takeda, S. and LaRoche, J.: Widespread Distribution and Expression of
668 Gamma A (UMB), an Uncultured, Diazotrophic, γ -Proteobacterial *nifH* Phylotype., *PLoS One*, 10(6), e0128912,
669 doi:10.1371/journal.pone.0128912, 2015.

670 Langlois, R. J., LaRoche, J. and Raab, P. a: Diazotrophic Diversity and Distribution in the Tropical and Subtropical
671 Atlantic Ocean Diazotrophic Diversity and Distribution in the Tropical and Subtropical Atlantic Ocean, *Appl.*
672 *Environ. Microbiol.*, 71(12), 7910–7919, doi:10.1128/AEM.71.12.7910, 2005.

673 Langlois, R. J., Hümmer, D. and LaRoche, J.: Abundances and distributions of the dominant *nifH* phylotypes in the
674 Northern Atlantic Ocean, *Appl. Environ. Microbiol.*, 74(6), 1922–1931, doi:10.1128/AEM.01720-07, 2008.

675 Lemaitre, N., Planchon, F., Planquette, H., Dehairs, F., Fonseca-Batista, D., Roukaerts, A., Deman, F., Tang, Y.,
676 Mariez, C. and Sarthou, G.: High variability of export fluxes along the North Atlantic GEOTRACES section
677 GA01: Particulate organic carbon export deduced from the ²³⁴Th method, *Biogeosciences Discuss.*, (April), 1–38,
678 doi:10.5194/bg-2018-190, 2018.

679 Li, X., Fonseca-Batista, D., Roevros, N., Dehairs, F. and Chou, L.: Environmental and nutrient controls of marine
680 nitrogen fixation, *Prog. Oceanogr.*, 167(August), 125–137, doi:10.1016/j.pocean.2018.08.001, 2018.

681 Loescher, C. R., Großkopf, T., Desai, F. D., Gill, D., Schunck, H., Croot, P. L., Schlosser, C., Neulinger, S. C.,
682 Pinnow, N., Lavik, G., Kuypers, M. M. M., Laroche, J. and Schmitz, R. A.: Facets of diazotrophy in the oxygen
683 minimum zone waters off Peru, *ISME J.*, 8(11), 2180–2192, doi:10.1038/ismej.2014.71, 2014.

684 Luo, H., Benner, R., Long, R. a and Hu, J.: Subcellular localization of marine bacterial alkaline phosphatases., *Proc.*
685 *Natl. Acad. Sci. U. S. A.*, 106(50), 21219–21223, doi:10.1073/pnas.0907586106, 2009.

686 Luo, Y.-W., Doney, S. C., Anderson, L. A., Benavides, M., Berman-Frank, I., Bode, A., Bonnet, S., Boström, K. H.,
687 Böttjer, D., Capone, D. G., Carpenter, E. J., Chen, Y. L., Church, M. J., Dore, J. E., Falcón, L. I., Fernández, A.,
688 Foster, R. A., Furuya, K., Gómez, F., Gundersen, K., Hynes, A. M., Karl, D. M., Kitajima, S., Langlois, R. J.,
689 LaRoche, J., Letelier, R. M., Marañón, E., McGillicuddy, D. J., Moisander, P. H., Moore, C. M., Mouriño-

690 Carballido, B., Mulholland, M. R., Needoba, J. A., Orcutt, K. M., Poulton, A. J., Rahav, E., Raimbault, P., Rees, A.
691 P., Riemann, L., Shiozaki, T., Subramaniam, A., Tyrrell, T., Turk-Kubo, K. A., Varela, M., Villareal, T. A., Webb,
692 E. A., White, A. E., Wu, J. and Zehr, J. P.: Database of diazotrophs in global ocean: abundance, biomass and
693 nitrogen fixation rates, *Earth Syst. Sci. Data*, 4(1), 47–73, doi:10.5194/essd-4-47-2012, 2012.

694 Luo, Y.-W., Lima, I. D., Karl, D. M., Deutsch, C. A. and Doney, S. C.: Data-based assessment of environmental
695 controls on global marine nitrogen fixation, *Biogeosciences*, 11(3), 691–708, doi:10.5194/bg-11-691-2014, 2014.

696 Man-Aharonovich, D., Kress, N., Zeev, E. B., Berman-Frank, I. and Béjà, O.: Molecular ecology of nifH genes and
697 transcripts in the eastern Mediterranean Sea, *Environ. Microbiol.*, 9(9), 2354–2363, doi:10.1111/j.1462-
698 2920.2007.01353.x, 2007.

699 Marañón, E., Holligan, P. M., Varela, M., Mouriño, B. and Bale, A. J.: Basin-scale variability of phytoplankton
700 biomass, production and growth in the Atlantic Ocean, *Deep Sea Res. Part I Oceanogr. Res. Pap.*, 47(5), 825–857,
701 doi:10.1016/S0967-0637(99)00087-4, 2000.

702 Martínez-Pérez, C., Mohr, W., Löscher, C. R., Dekaezemacker, J., Littmann, S., Yilmaz, P., Lehnen, N., Fuchs, B.
703 M., Lavik, G., Schmitz, R. A., LaRoche, J. and Kuypers, M. M. M.: The small unicellular diazotrophic symbiont,
704 UCYN-A, is a key player in the marine nitrogen cycle, *Nat. Microbiol.*, 1(September), 1–7,
705 doi:10.1038/nmicrobiol.2016.163, 2016.

706 McCartney, M. S. and Talley, L. D.: The Subpolar Mode Water of the North Atlantic Ocean, *J. Phys. Oceanogr.*,
707 12(11), 1169–1188, doi:10.1175/1520-0485(1982)012<1169:TSMWOT>2.0.CO;2, 1982.

708 Mills, M. M., Ridame, C., Davey, M., La Roche, J. and Geider, R. J.: Iron and phosphorus co-limit nitrogen fixation
709 in the eastern tropical North Atlantic, *Nature*, 429(May), 292–294, doi:10.1038/nature02550, 2004.

710 Mohr, W., Großkopf, T., Wallace, D. W. R. and LaRoche, J.: Methodological underestimation of oceanic nitrogen
711 fixation rates, *PLoS One*, 5(9), 1–7, doi:10.1371/journal.pone.0012583, 2010.

712 Montoya, J. P., Voss, M., Kahler, P. and Capone, D. G.: A Simple, High-Precision, High-Sensitivity Tracer Assay for
713 N₂ Fixation, *Appl. Environ. Microbiol.*, 62(3), 986–993, 1996.

714 Montoya, J. P., Voss, M. and Capone, D. G.: Spatial variation in N₂-fixation rate and diazotroph activity in the
715 Tropical Atlantic, *Biogeosciences*, 4(3), 369–376, doi:10.5194/bg-4-369-2007, 2007.

716 Moore, C. M., Mills, M. M., Achterberg, E. P., Geider, R. J., LaRoche, J., Lucas, M. I., McDonagh, E. L., Pan, X.,
717 Poulton, A. J., Rijkenberg, M. J. A., Suggett, D. J., Ussher, S. J. and Woodward, E. M. S.: Large-scale distribution
718 of Atlantic nitrogen fixation controlled by iron availability, *Nat. Geosci.*, 2(12), 867–871, doi:10.1038/ngeo667,
719 2009.

720 Moreira-Coello, V., Mouriño-Carballido, B., Marañón, E., Fernández-Carrera, A., Bode, A. and Varela, M. M.:
721 Biological N₂ Fixation in the Upwelling Region off NW Iberia: Magnitude, Relevance, and Players, *Front. Mar.*
722 *Sci.*, 4(September), doi:10.3389/fmars.2017.00303, 2017.

723 Mulholland, M. R., Bernhardt, P. W., Blanco-Garcia, J. L., Mannino, A., Hyde, K., Mondragon, E., Turk, K.,
724 Moisander, P. H. and Zehr, J. P.: Rates of dinitrogen fixation and the abundance of diazotrophs in North American
725 coastal waters between Cape Hatteras and Georges Bank, *Limnol. Oceanogr.*, 57(4), 1067–1083,
726 doi:10.4319/lo.2012.57.4.1067, 2012.

727 Needoba, J. A., Foster, R. A., Sakamoto, C., Zehr, J. P. and Johnson, K. S.: Nitrogen fixation by unicellular
728 diazotrophic cyanobacteria in the temperate oligotrophic North Pacific Ocean, *Limnol. Oceanogr.*, 52(4), 1317–
729 1327, doi:10.4319/lo.2007.52.4.1317, 2007.

730 Nei, M.: *Molecular Evolutionary Genetics*, Columbia University Press, New York, United States, 1987.

731 Ohlendieck, U., Stuhr, A. and Siegmund, H.: Nitrogen fixation by diazotrophic cyanobacteria in the Baltic Sea and
732 transfer of the newly fixed nitrogen to picoplankton organisms, *J. Mar. Syst.*, 25(3–4), 213–219,
733 doi:10.1016/S0924-7963(00)00016-6, 2000.

734 Poulton, A. J., Holligan, P. M., Hickman, A., Kim, Y. N., Adey, T. R., Stinchcombe, M. C., Holeton, C., Root, S. and
735 Woodward, E. M. S.: Phytoplankton carbon fixation, chlorophyll-biomass and diagnostic pigments in the Atlantic
736 Ocean, *Deep. Res. Part II Top. Stud. Oceanogr.*, 53(14–16), 1593–1610, doi:10.1016/j.dsr2.2006.05.007, 2006.

737 Rahav, E., Bar-Zeev, E., Ohayon, S., Elifantz, H., Belkin, N., Herut, B., Mulholland, M. R. and Berman-Frank, I.:
738 Dinitrogen fixation in aphotic oxygenated marine environments, *Front. Microbiol.*, 4(AUG), 1–11,
739 doi:10.3389/fmicb.2013.00227, 2013.

740 Rahav, E., Giannetto, M. J. and Bar-Zeev, E.: Contribution of mono and polysaccharides to heterotrophic N₂ fixation
741 at the eastern Mediterranean coastline, *Sci. Rep.*, 6(May), 1–11, doi:10.1038/srep27858, 2016.

742 Ratten, J.-M.: The diversity, distribution and potential metabolism of non-cyanobacterial diazotrophs in the North
743 Atlantic Ocean, Dalhousie University., 2017.

744 Ratten, J. M., LaRoche, J., Desai, D. K., Shelley, R. U., Landing, W. M., Boyle, E., Cutter, G. A. and Langlois, R. J.:
745 Sources of iron and phosphate affect the distribution of diazotrophs in the North Atlantic, *Deep. Res. Part II Top.*
746 *Stud. Oceanogr.*, 116, 332–341, doi:10.1016/j.dsr2.2014.11.012, 2015.

747 Raven, J. A.: The iron and molybdenum use efficiencies of plant growth with different energy, carbon and nitrogen
748 sources, *New Phytol.*, 109, 279–287, doi:10.1111/j.1469-8137.1988.tb04196.x, 1988.

749 Rees, A., Gilbert, J. and Kelly-Gerreyn, B.: Nitrogen fixation in the western English Channel (NE Atlantic Ocean),
750 *Mar. Ecol. Prog. Ser.*, 374(1979), 7–12, doi:10.3354/meps07771, 2009.

751 Rijkenberg, M. J. A., Langlois, R. J., Mills, M. M., Patey, M. D., Hill, P. G., Nielsdóttir, M. C., Compton, T. J.,
752 LaRoche, J. and Achterberg, E. P.: Environmental forcing of nitrogen fixation in the Eastern Tropical and Sub-
753 Tropical North Atlantic Ocean, *PLoS One*, 6(12), doi:10.1371/journal.pone.0028989, 2011.

754 Riou, V., Fonseca-Batista, D., Roukaerts, A., Biegala, I. C., Prakya, S. R., Magalhães Loureiro, C., Santos, M.,
755 Muniz-Piniella, A. E., Schmiing, M., Elskens, M., Brion, N., Martins, M. A. and Dehairs, F.: Importance of N₂-
756 Fixation on the Productivity at the North-Western Azores Current/Front System, and the Abundance of
757 Diazotrophic Unicellular Cyanobacteria, *PLoS One*, 11(3), e0150827, doi:10.1371/journal.pone.0150827, 2016.

758 Sarthou, G., Baker, A. R., Blain, S., Achterberg, E. P., Boye, M., Bowie, A. R., Croot, P., Laan, P., De Baar, H. J.
759 W., Jickells, T. D. and Worsfold, P. J.: Atmospheric iron deposition and sea-surface dissolved iron concentrations
760 in the eastern Atlantic Ocean, *Deep. Res. Part I Oceanogr. Res. Pap.*, 50(10–11), 1339–1352, doi:10.1016/S0967-
761 0637(03)00126-2, 2003.

762 Scavotto, R. E., Dziallas, C., Bentzon-Tilia, M., Riemann, L. and Moisaner, P. H.: Nitrogen-fixing bacteria
763 associated with copepods in coastal waters of the North Atlantic Ocean, *Environ. Microbiol.*, 17(10), 3754–3765,
764 doi:10.1111/1462-2920.12777, 2015.

765 Shelley, R. U., Roca-Martí, M., Castrillejo, M., Sanial, V., Masqué, P., Landing, W. M., van Beek, P., Planquette, H.
766 and Sarthou, G.: Quantification of trace element atmospheric deposition fluxes to the Atlantic Ocean (> 40°N;
767 GEOVIDE, GEOTRACES GA01) during spring 2014, *Deep. Res. Part I*, 119(November 2016), 34–49,
768 doi:10.1016/j.dsr.2016.11.010, 2017.

769 Shiozaki, T., Ijichi, M., Kodama, T., Takeda, S., Furuya, K., Ijichi, M., Kodama, T., Takeda, S. and Furuya, K.:
770 Heterotrophic bacteria as major nitrogen fixers in the euphotic zone of the Indian Ocean, *Global Biogeochem.*
771 *Cycles*, 28, 1096–1110, doi.org/10.1002/2014GB004886, 2014.

772 Shiozaki, T., Nagata, T., Ijichi, M. and Furuya, K.: Nitrogen fixation and the diazotroph community in the temperate
773 coastal region of the northwestern North Pacific, *Biogeosciences*, 12(15), 4751–4764, doi:10.5194/bg-12-4751-
774 2015, 2015.

775 Snow, J. T., Schlosser, C., Woodward, E. M. S., Mills, M. M., Achterberg, E. P., Mahaffey, C., Bibby, T. S. and
776 Moore, C. M.: Environmental controls on the biogeography of diazotrophy and *Trichodesmium* in the Atlantic
777 Ocean, *Global Biogeochem. Cycles*, 29, 865–884, doi.org/10.1002/2015GB005090, 2015.

778 Subramaniam, A., Yager, P. L., Carpenter, E. J., Mahaffey, C., Björkman, K., Cooley, S., Kustka, A. B., Montoya, J.
779 P., Sañudo-Wilhelmy, S. A., Shipe, R. and Capone, D. G.: Amazon River enhances diazotrophy and carbon
780 sequestration in the tropical North Atlantic Ocean, *Global Biogeochem. Cycles*, 105, 10460–10465,
781 doi:10.1029/2006GB002751, 2008.

782 Subramaniam, A., Mahaffey, C., Johns, W. and Mahowald, N.: Equatorial upwelling enhances nitrogen fixation in
783 the Atlantic Ocean, *Geophys. Res. Lett.*, 40(9), 1766–1771, doi:10.1002/grl.50250, 2013.

784 Thompson, A. W., Foster, R. A., Krupke, A., Carter, B. J., Musat, N., Vaultot, D., Kuypers, M. M. M. and Zehr, J. P.:
785 Unicellular Cyanobacterium Symbiotic with a Single-Celled Eukaryotic Alga, *Science*, 337(September), 1546–
786 1550, 2012.

787 Thuróczy, C.-E., Gerringa, L. J. A., Klunder, M. B., Middag, R., Laan, P., Timmermans, K. R. and de Baar, H. J. W.:
788 Speciation of Fe in the Eastern North Atlantic Ocean, *Deep Sea Res. Part I Oceanogr. Res. Pap.*, 57(11), 1444–
789 1453, doi:10.1016/j.dsr.2010.08.004, 2010.

790 Tonnard, M., Planquette, H., Bowie, A. R., van der Merwe, P., Gallinari, M., Deprez de Gesincourt, F., Germain, Y.,
791 Gourain, A., Benetti, M., Reverdin, G., Treguer, P., Boutorh, J., Cheize, M., Menzel Barraqueta, J.-L., Pereira-
792 Contraira, L., Shelley, R., Lherminier, P. and Sarthou, G.: Dissolved iron distribution in the North Atlantic Ocean
793 and Labrador Sea along the GEOVIDE section (GEOTRACES section GA01), *Biogeosciences Discuss.*, (April),
794 2018.

795 Vidal, M., Duarte, C. M. and Agustí, S.: Dissolved organic nitrogen and phosphorus pools and fluxes in the central
796 Atlantic Ocean, *Limnol. Oceanogr.*, 44(1), 106–115, 1999.

797 Vidal, M., Duarte, C. M., Agustí, S., Gasol, J. M. and Vaqué, D.: Alkaline phosphatase activities in the central
798 Atlantic Ocean indicate large areas with phosphorus deficiency, *Mar. Ecol. Prog. Ser.*, 262, 43–53,
799 doi:10.3354/meps262043, 2003.

800 Villa-Alfageme, M., de Soto, F. C., Ceballos, E., Giering, S. L. C., Le Moigne, F. A. C., Henson, S., Mas, J. L. and
801 Sanders, R. J.: Geographical, seasonal, and depth variation in sinking particle speeds in the North Atlantic,
802 *Geophys. Res. Lett.*, 43, 8609–8616, doi.org/10.1002/2016GL069233, 2016.

803 Voss, M., Croot, P., Lochte, K., Mills, M. and Peeken, I.: Patterns of nitrogen fixation along 10°N in the tropical
804 Atlantic, *Geophys. Res. Lett.*, 31(23), 1–4, doi:10.1029/2004GL020127, 2004.

805 Wertz, J. T., Kim, E., Breznak, J. A., Schmidt, T. M. and Rodrigues, J. L. M.: Genomic and physiological
806 characterization of the Verrucomicrobia isolate *Diplosphaera colitermitum* gen. nov., sp. nov., reveals
807 microaerophily and nitrogen fixation genes, *Appl. Environ. Microbiol.*, 78(5), 1544–1555,
808 doi:10.1128/AEM.06466-11, 2012.

809 Yentsch, C. S. and Menzel, D. W.: A method for the determination of phytoplankton chlorophyll and phaeophytin by
810 fluorescence, *Deep Sea Res. Oceanogr. Abstr.*, 10(3), 221–231, doi:10.1016/0011-7471(63)90358-9, 1963.

811 Zani, S., Mellon, M. T., Collier, J. L. and Zehr, J. P.: Expression of *nifH* genes in natural microbial assemblages in
812 Lake George, New York, detected by reverse transcriptase PCR, *Appl. Environ. Microbiol.*, 66(7), 3119–3124,
813 doi:10.1128/AEM.66.7.3119-3124.2000, 2000.

814 **Tables**

815

816

817 **Table 1:** Relative contribution (%) of N₂ fixation to Primary Production (PP).

Province	Station	Latitude (° N)	Longitude (° E)	N ₂ fixation contribution to PP (%) (Redfield 6.6 ratio)	SD	N ₂ fixation contribution to PP (%) (mean POC/PN ratio of 6.3 ± 1.1)	SD
ENACW _{sp}	Bel-3	46.5	-8.0	0	-	0	-
	Bel-5	45.3	-8.8	0	-	0	-
	Bel-7	44.6	-9.3	2	0.4	1	0.4
	Geo-21	46.5	-19.7	1	0.02	1	0.0
ENACW _{st}	Bel-9	42.4	-9.7	1	0.1	1	0.1
	Bel-11	40.7	-11.1	28	1.9	25	1.8
	Bel-13	38.8	-11.4	25	1.3	23	1.2
	Geo-1	40.3	-10.0	3	0.2	3	0.1
	Geo-2	40.3	-9.5	3	0.1	3	0.1
	Geo-13	41.4	-13.9	3	0.1	3	0.1

818

819 **Figure legends**

820 **Figure 1:** Location of sampling stations during the Belgica BG2014/14 (black labels) and GEOVIDE (white labels)
821 cruises (May 2014) superimposed on a map of the seasonal average phosphate excess ($P^* = [\text{PO}_4^{3-}] - [\text{NO}_3^-] / 16$) at
822 20 m (April to June for the period from 1955 to 2012; World Ocean Atlas 2013; Garcia et al., 2013). Areas of
823 dominance of the Eastern North Atlantic Central Waters of subpolar (ENACWsp) and subtropical (ENACWst) origin
824 are separated by a horizontal dashed line. Black dashed and solid contour lines illustrate 500 m and 1500 m isobaths,
825 respectively. (Schlitzer, R., Ocean Data View).

826

827 **Figure 2:** Spatial distribution of Chl *a* (**a, d**), NH_4^+ (**b, e**) and $\text{NO}_3^- + \text{NO}_2^-$ (**c, f**) concentrations along the Belgica
828 BG2014/14 (**upper panels**) and GEOVIDE (**lower panels**) cruise tracks. Station numbers are indicated above the
829 sections. The vertical black line represents the boundary between areas with dominance of Eastern North Atlantic
830 Waters of subpolar (ENACWsp) and subtropical (ENACWst) origin. Mixed layer depth (MLD, black lines
831 connecting diamonds) was estimated using a temperature threshold criterion of 0.2°C relative to the temperature at 10
832 m (de Boyer Montégut et al., 2004). (Schlitzer, R., Ocean Data View).

833

834 **Figure 3:** Spatial distribution (\pm SD) of depth-integrated rates of primary production (**a, b**) (duplicates are in light
835 and dark green bars with the corresponding values in $\text{mmol C m}^{-2} \text{d}^{-1}$); N_2 fixation (**c, d**) (duplicates are in light and
836 dark blue bars with the corresponding values in $\mu\text{mol N m}^{-2} \text{d}^{-1}$) determined during the Belgica BG2014/14 (**a, c**) and
837 GEOVIDE (**b, d**) cruises. Error bars represent the propagated measurement uncertainty of all parameters used to
838 compute volumetric uptake rates.

839

840 **Figure 4:** Time series of area-averaged chlorophyll *a* concentration (mg m^{-3}) registered by Aqua MODIS satellite
841 (Giovanni online satellite data system) between December 2013 and December 2014 for the $0.5^\circ \times 0.5^\circ$ grid
842 surrounding the different stations during the (**a**) Belgica BG2014/14 and (**b**) GEOVIDE cruises. The dashed box
843 highlights the sampling period for both cruises (May 2014).

844

845 **Figure 5:** Diversity of *nifH* sequences during (**a**) the Belgica BG2014/14 cruise (successfully recovered only at
846 stations Bel-11 and Bel-13, 5 m) and (**b**) the GEOVIDE cruise (stations Geo-2, 100 m; Geo-13, 35 m and Geo-21, 15
847 and 70 m). The total numbers of recovered sequences are indicated on top of the bars, and the exact percentage
848 represented by each group is shown inside the bars.

849

850 **Figure 6:** Phylogenetic tree of *nifH* predicted amino acid sequences generated using the Maximum Likelihood
851 method of the Kimura 2-parameter model (Kimura, 1980) via the Molecular Evolutionary Genetics Analysis software
852 (MEGA 7.0) (Kumar et al., 2016). Initial tree(s) for the heuristic search were obtained automatically by applying
853 Neighbor-Join and BioNJ algorithms to a matrix of pairwise distances estimated using the Maximum Composite
854 Likelihood (MCL) approach, and then selecting the topology with superior log likelihood value. A discrete Gamma
855 distribution was used to model evolutionary rate differences among sites (5 categories (+G, parameter = 0.4038)). All
856 sequences recovered from DNA samples, including those previously identified and the newly recovered ones (with \geq
857 95% similarity at the nucleotide level with representative clones) are highlighted in blue. For the *nifH* sequences
858 recovered from the GEOVIDE cruise, only those contributing to the cumulative 98% of recovered sequences were
859 included in this tree. Bootstrap support values (\geq 50%) for 100 replications are shown at nodes. The scale bar

860 indicates the number of sequence substitutions per site. The archaean *Methanobrevibacter smithii* was used as an
861 outgroup. Accession numbers for published sequences used to construct the phylogenetic tree are given.

862

863 **Figure 7:** Euclidean distance biplot illustrating the axis loadings for the two main PCA components based on the
864 Spearman rank correlation matrix shown in Table S3. Variables taken into account include depth-integrated rates of
865 N₂ fixation and primary production (PP), average phosphate excess at 20 m depth surrounding each sampled site
866 recovered from World Ocean Atlas 2013 climatology data between April and June from 1955 to 2012 (Garcia et al.,
867 2013); satellite average dust deposition (dry + wet) derived during April 2014 (Giovanni online data system, NASA
868 Goddard Earth Sciences Data and Information Services Center) and ambient variables (temperature, salinity, and
869 nutrient data). Coloured dots in the biplot represent the projection of the different stations. Axis 1 has high negative
870 loadings for PP, Chl *a*, NH₄⁺ and NO₃⁻ + NO₂⁻, and high positive loadings for temperature and N₂ fixation rates, with
871 values of -0.812, -0.768, -0.936, -0.783, 0.942 and 0.506, respectively (see Table S5). Axis 2 has high positive
872 loadings of 0.584, 0.943 and 0.602 for climatological P*, salinity and N₂ fixation rates, respectively. PCA analysis
873 was run in XLSTAT 2017 (Addinsoft, Paris, France, 2017).

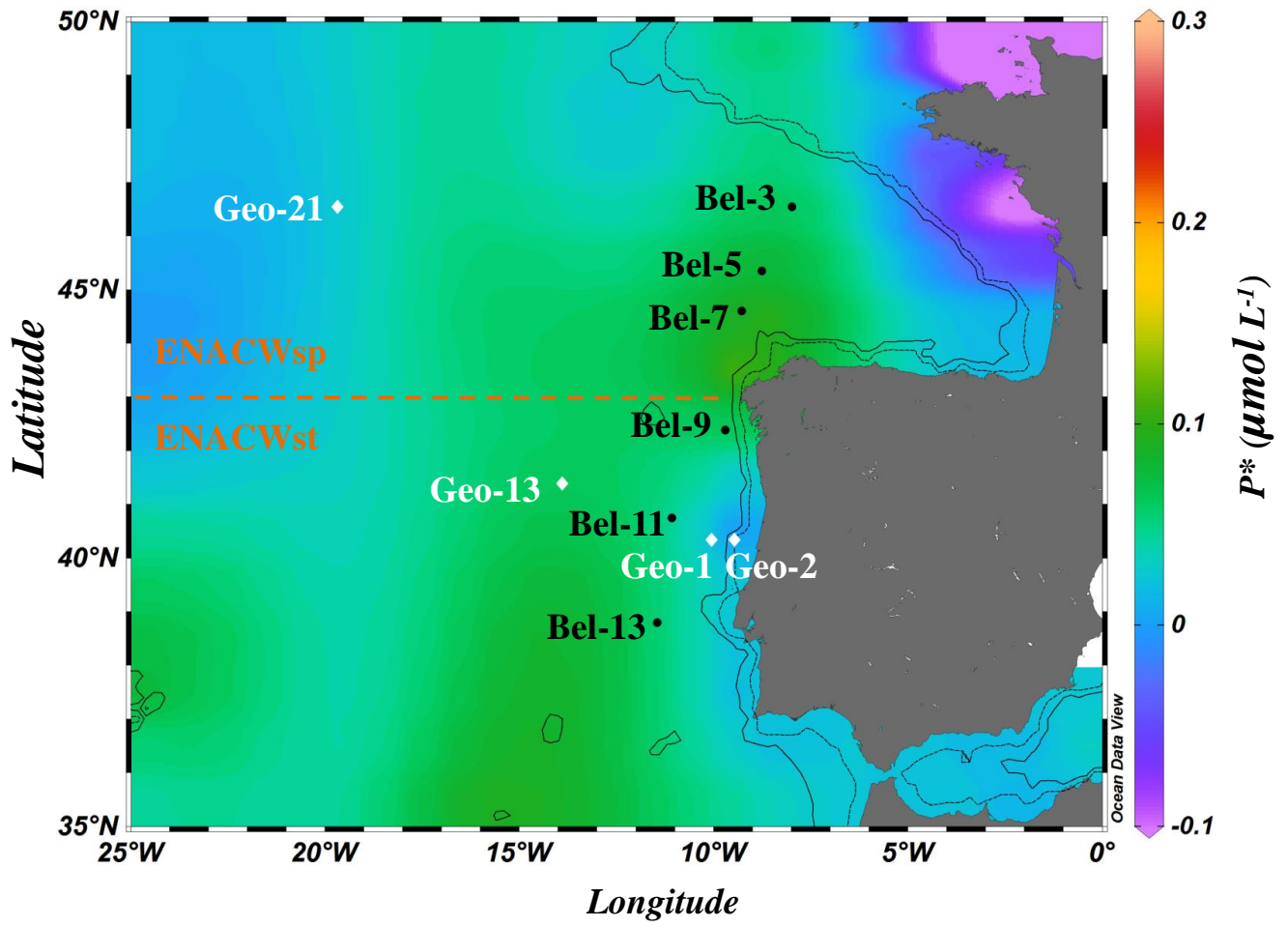
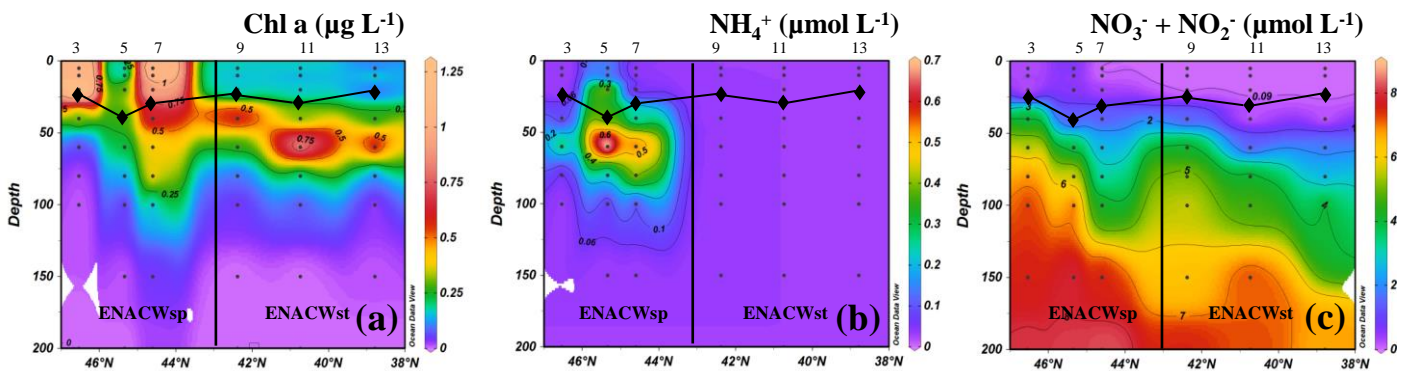


Figure 1

Belgica BG2014/14



GEOVIDE

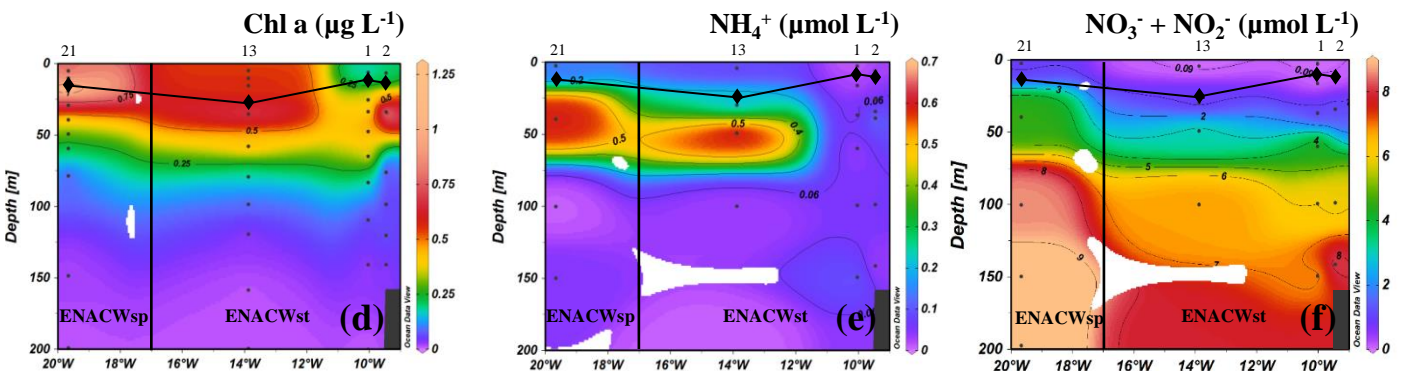


Figure 2

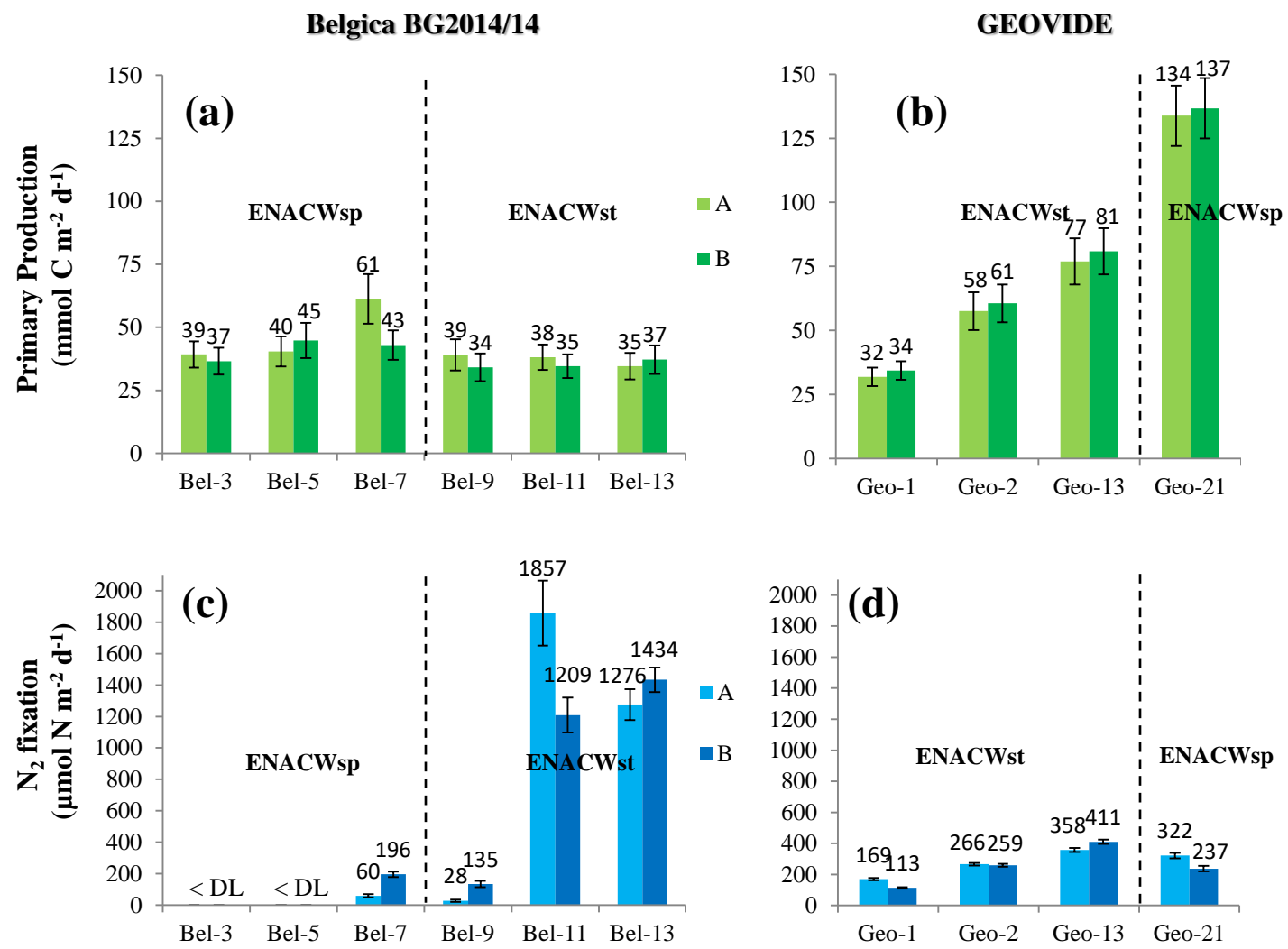


Figure 3

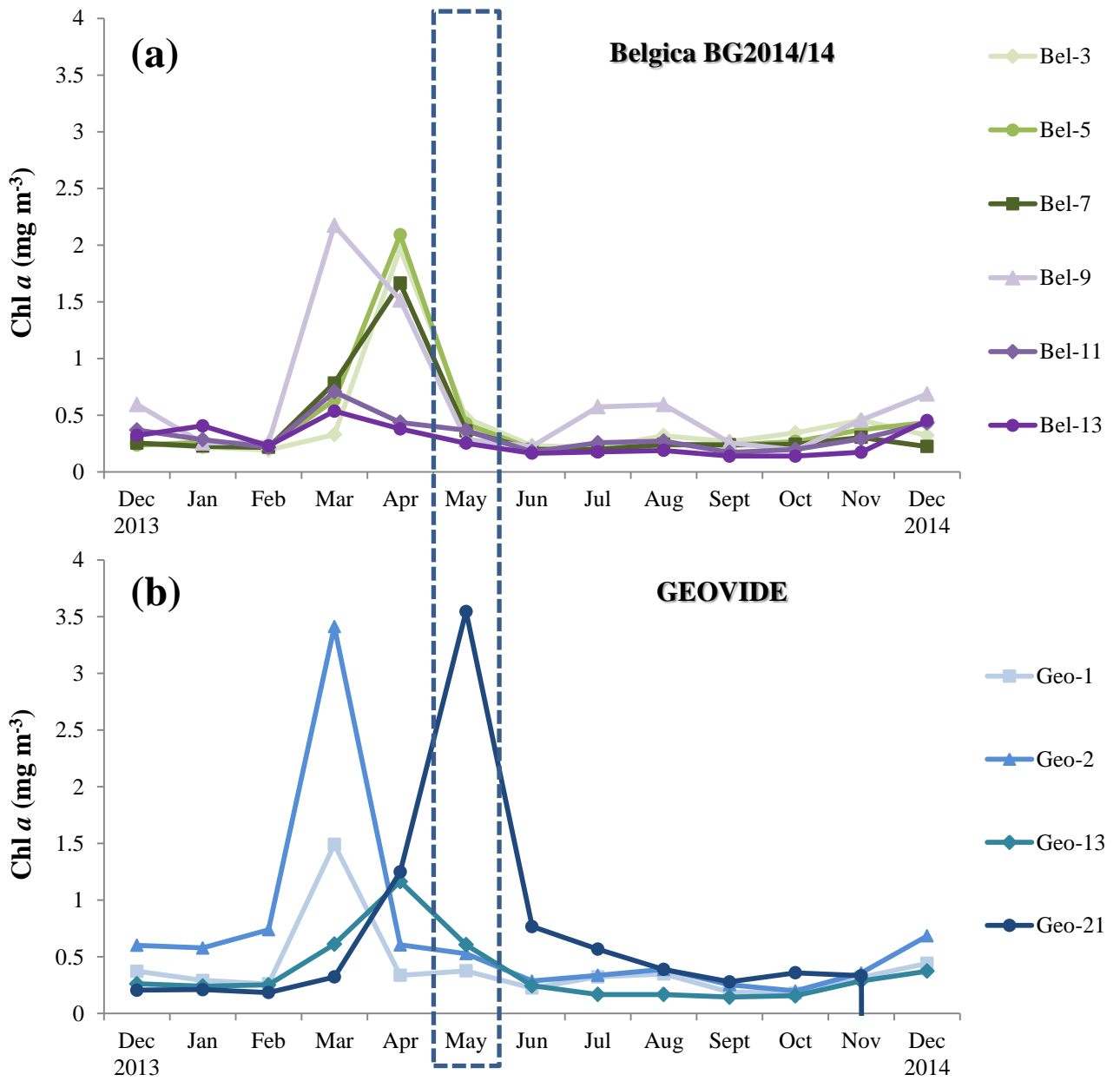


Figure 4

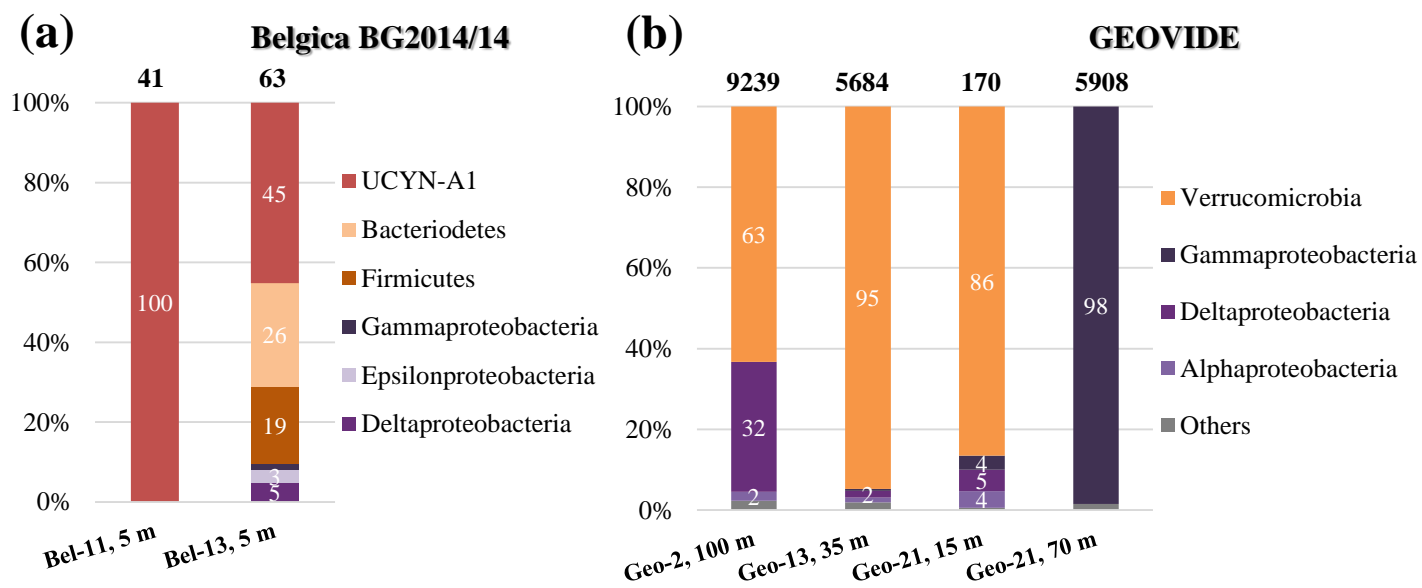


Figure 5

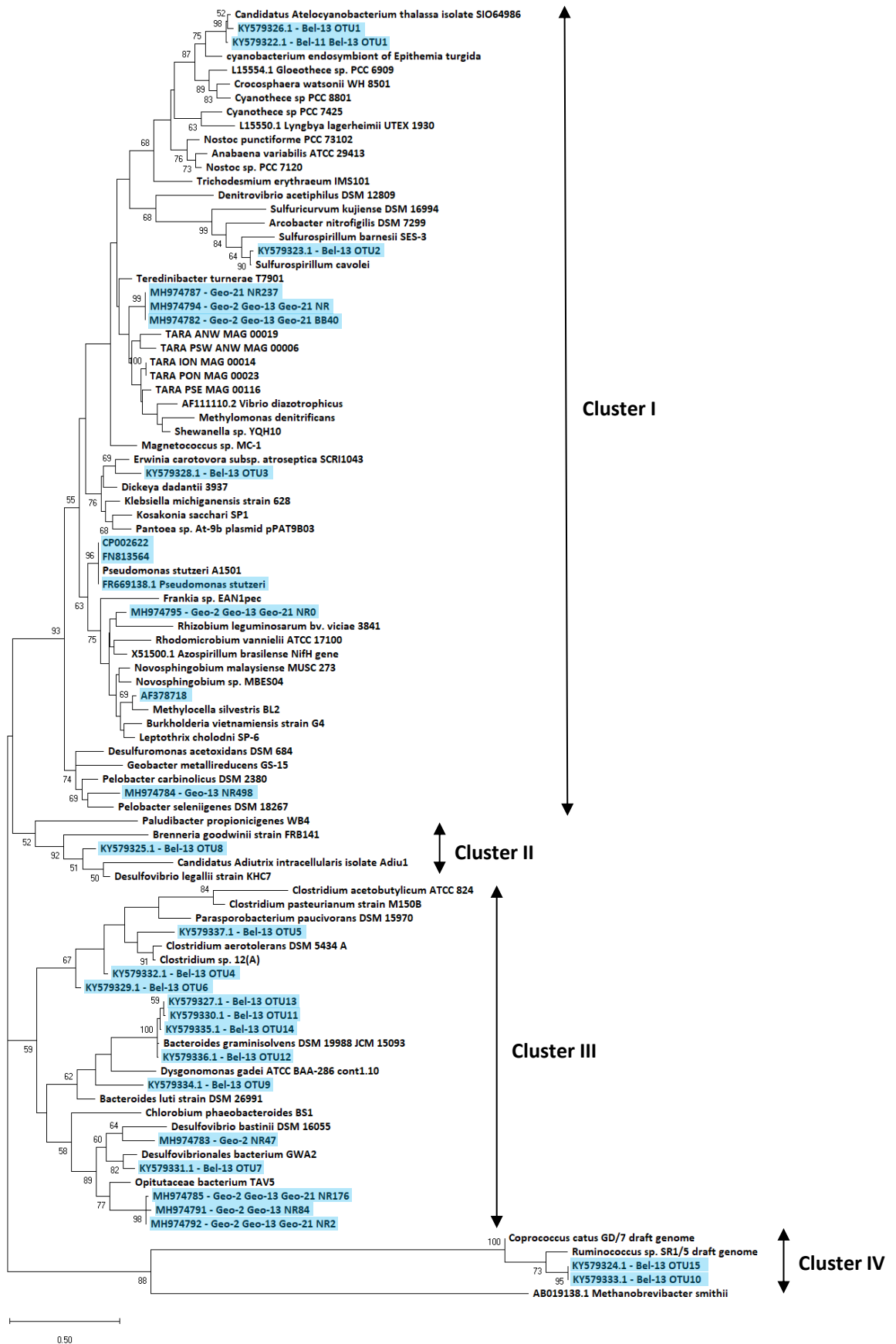


Figure 6

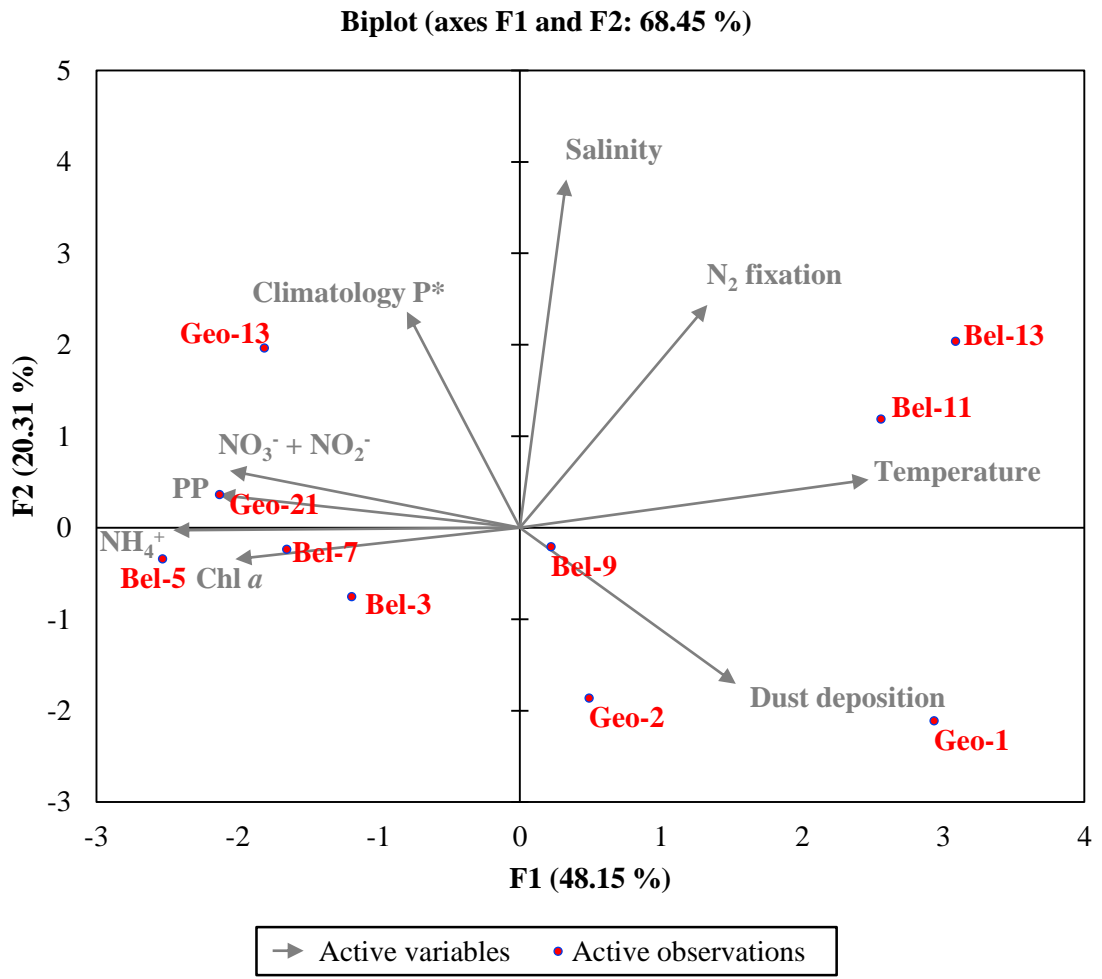


Figure 7